[5–8]. It has been suggested that this association may be population specific [9], and highly influenced by environmental factors, such as alcohol consumption, tobacco smoking, and body mass index (BMI) [5,10–12]. Moreover, an interaction between the *Taq*IB genotypes and the progression of CHD after therapy has been shown [13]. These observations could be significantly relevant because low plasma HDL cholesterol levels are associated with an increase in the risk of CHD [14]. Therefore, CETP could have a relevant role in atherogenesis through its effects on HDL metabolism.

The aim of the present study was to determine the gene-environmental interaction in the regulation of plasma HDL cholesterol levels in the Japanese general population, which has higher alcohol intake and higher smoking rates in men and lower alcohol intake and lower smoking rates in women than the Caucasian population [15]. In the present study, we analyzed the association among the CETP *Taq*IB polymorphism, HDL cholesterol levels, and gene-environmental interaction in a population-based sample of Japanese men and women.

2. Methods

2.1. Population

The selection criteria and design of this study have been previously described [16–18]. We conducted this study in S town, a rural farming mountain area near Kyoto in the western part of Japan, which had a population of about 15,000. Among the 2892 residents who underwent medical check-ups in 1999, a total of 2395, with 917 men (mean age ± S.D., 58.0 ± 15.7) and 1478 women (mean age ± S.D., 56.3 ± 15.6), were enrolled after a full explanation of this genetic study was given and informed consent was obtained. Of these, a total of 666 were excluded because their genotype was not determined (175 men, 255 women), they were taking lipid-lowering medications (41 men, 109 women), or they had a history of coronary heart disease or stroke (42 men, 44 women). After this exclusion, 1729 participants (659 men, 1070 women) were studied. This study received approval of the Institutional Review Board of Shiga University of Medical Science.

2.2. Genetic analysis

DNA was isolated from peripheral leukocytes according to standard procedures. We analyzed the *Taq*IB polymorphism, which has been shown to be a silent base change affecting the 277th nucleotide in the first intron of the CETP gene. The B1 allele indicates the presence of the *Taq*I restriction site and the B2 allele represents the absence of the *Taq*I restriction site. The *Taq*IB polymorphism was genotyped using the polymerase chain reaction-restriction fragment length polymorphism (PCR-RFLP) analysis method described previously [11]. The designed primers were 5′-CACTAGCCCAGAGAGAGGAGTGCC-3′ (sense) and 5′-CTGAGCCCAGCCGCACACTAAC-3′ (antisense). DNA templates were denatured at 95 °C for 3 min, and then each PCR reaction was subjected to 30 cycles with a temperature cycle consisting of 95 °C for 30 s, 60 °C for 30 s, and 72 °C for 45 s, and finally an extension at 72 °C for 5 min on a GeneAmp PCR System 9700 (Applied Biosystems, Foster City, CA, USA). The amplified fragments were digested with *Taq*I restriction enzyme (New England Biolabs, Beverly, Massachusetts, USA) and subjected to electrophoresis on 1.5% agarose gels. The resulting fragments were 174 bp and 361 bp for the B1 allele and 535 bp for the uncut B2 allele. Genotypes, determined by the PCR-RFLP method on a total of 75 random samples consisting of 25 PCR products of each genotype, were confirmed by direct sequencing. Briefly, after fractionation of PCR-RFLP products on 1% agarose gels, the desired DNA bands were cut out, and the DNA was purified using a QIAquick Gel Extraction Kit (QIAGEN, Valencia, California, USA) and was amplified with the above 5′ primer, followed by analysis on an ABI PRISM 310 Genetic Analyzer (Applied Biosystems).

2.3. Measurements

Non-fasting blood was drawn and serum total cholesterol (T-CHO) and HDL cholesterol levels were determined in a laboratory (Medic, Shiga, Japan). The measurement precision and accuracy of these serum lipids were certified through a lipid standardization program by Osaka Medical Center for Cancer and Cardiovascular Diseases, which is a member of Cholesterol Reference Method Laboratory Network (CRMLN) controlled by the Centers for Disease Control and Prevention (Atlanta, GA, USA) [19]. Hypertension was defined as a systolic blood pressure of ≥140 mmHg, or a diastolic blood pressure of ≥90 mmHg, or current use of antihypertensive drugs. Diabetes mellitus was defined as a non-fasting blood glucose ≥11.1 mmol/L (200 mg/dL) or current use of diabetic drugs or insulin infusion.

2.4. Information on alcohol drinking and smoking habit

Using a questionnaire, a well-trained public health nurse obtained information on alcohol drinking and smoking habits [16,18]. The average frequency of drinking per week and the average alcohol intake on each occasion were determined, and the alcohol consumption per week was calculated, which was then divided by 7 to give the alcohol consumption per day. One drink unit was defined as 11.5 g of ethanol per day, which was equal to a half go (90 mL) of sake, one bottle (350 mL) of beer, one single whiskey, or one glass (120 mL) of wine. Drinkers were defined as those who drank any alcohol. We checked whether the participants currently smoked (current smoker), whether the participants had a history of smoking (smoking history), and how many cigarettes the participants smoked per day.

2.5. Statistical analyses

All analyses were performed separately for men and women. Deviation from Hardy–Weinberg equilibrium was examined by χ^2-analysis. Characteristics of participants were analyzed by the genotypes of the *Taq*IB polymorphism as follows: differences in frequencies were examined by χ^2 analysis and differences in quantitative variables were examined by one-way analysis of variance (ANOVA) and Tukey post-hoc test for multiple comparisons. To examine whether the *Taq*IB genotype (B1B1 or B1B2 = 0, B2B2 = 1) is an independent determinant of HDL cholesterol levels, multiple regression analyses were performed using two models. Model 1 was done with other covariates (age, waist to hip [W/H] ratio, alcohol drinking [non-drinker = 0, drinker = 1], current smoking [non-smoker = 0, smoker = 1], non-HDL cholesterol, and logarithm of triglyceride [TG]). Model 2 was done with the same covariates as model 1 plus interaction between the *Taq*IB genotype and W/H ratio, alcohol drinking, or current smoking. Because TG distribution was not a normal distribution, we used the logarithm of TG values. To assess the interaction between alcohol consumption, current smoking status, BMI, or W/H ratio and the CETP *Taq*IB polymorphism in the regulation of HDL cholesterol levels, analysis of covariance (ANCOVA) was used. Since the average levels of alcohol consumption were much lower among women than men, alcohol consumption was categorized as more than 2 drinks/day for men and any alcohol consumption for women. All statistical analyses were performed using the JMP statistical software package (SAS Institute Inc., Cary, NC, USA).

3. Results

The clinical characteristics of participants were analyzed according to the *Taq*IB genotype for men and women (Table 1). The allele frequencies for the B1 (95% confidence interval) was as follows: in men, 59.9% (57.2–62.5%); in women, 60.0% (58.0–62.0%); and overall, 59.9% (58.3–61.6%). The observed genotype frequencies were in agreement with those predicted by Hardy–Weinberg equilibrium. No gender differences in genotype or allele distribution were observed.

A comparison among the *Taq*IB genotypes in men showed significant differences in the percentage of current smokers and smoking history. HDL cholesterol level in the B2B2 genotype tended to be higher than the B1B1 genotype. In women, a comparison among the *Taq*IB genotypes showed significant differences in age, HDL cholesterol, and non-HDL cholesterol levels. HDL cholesterol level in the B2B2 genotype was significantly higher than those in the other genotypes. Non-HDL cholesterol level in the B2B2 genotype was significantly lower than that in the B1B1 genotype.

Table 2 shows the results of multivariate regression analyses of determinants for HDL cholesterol levels in the participants. Model 1 was done with the *Taq*IB genotypes and other covariates. Because BMI was strongly associated with

Table 1
Characteristics of the participants according to CETP Taq IB genotype in 1999, Shiga, Japan

Characteristics	Men				Women			
	CETP *Taq* IB genotype			*p*-value	CETP *Taq* IB genotype			*p*-value
	B1B1	B1B2	B2B2		B1B1	B1B2	B2B2	
Number	234	321	104		377	530	163	
Genotype frequency (%)	35.5	48.7	15.8		35.2	49.5	15.2	
Age (years)	57.5 ± 15.9	57.2 ± 16.2	58.9 ± 13.6	0.621	55.2 ± 15.6	56.2 ± 15.1	52.1 ± 17.3#	0.016
Body mass index (kg/m^2)	22.6 ± 3.1	22.5 ± 2.8	22.7 ± 3.3	0.763	22.4 ± 3.2	22.4 ± 3.3	22.1 ± 3.1	0.533
Waist to hip ratio	0.88 ± 0.07	0.87 ± 0.07	0.87 ± 0.07	0.726	0.78 ± 0.06	0.79 ± 0.06	0.78 ± 0.06	0.100
Alcohol consumption (g/day)	22.2 ± 19.7	19.5 ± 19.7	23.5 ± 20.2	0.108	3.0 ± 6.8	2.7 ± 6.3	3.6 ± 7.1	0.350
Drinker (%)	76.9	70.4	76.9	0.164	26.8	23.8	30.7	0.193
Smoking consumption (cigarettes/day)	11.4 ± 12.5	11.2 ± 13.4	8.5 ± 12.1	0.136	0.7 ± 3.0	0.8 ± 3.8	0.6 ± 2.9	0.803
Current smoker (%)	54.3	53.3	40.4	0.043	6.6	5.9	6.1	0.891
Smoking history (%)	82.5	80.4	65.4	0.002	9.3	8.1	8.6	0.826
Hypertension (%)	41.9	41.4	38.8	0.865	32.9	35.9	35.6	0.624
Diabetes mellitus (%)	3.9	6.5	3.9	0.292	2.7	2.8	1.8	0.770
Total cholesterol (mmol/L)	4.71 ± 0.79	4.77 ± 0.90	4.78 ± 0.97	0.647	5.12 ± 0.88	5.05 ± 0.89	5.01 ± 0.88	0.323
Triglycerides (mmol/L)	1.71 ± 1.19	1.65 ± 1.17	1.64 ± 1.07	0.795	1.30 ± 0.82	1.28 ± 0.69	1.22 ± 0.71	0.502
HDL cholesterol (mmol/L)	1.33 ± 0.34	1.36 ± 0.36	1.42 ± 0.40	0.096	1.53 ± 0.36	1.58 ± 0.36	1.69 ± 0.38*,#	< 0.001
Non-HDL cholesterol (mmol/L)	3.38 ± 0.84	3.41 ± 0.89	3.36 ± 0.99	0.839	3.59 ± 0.91	3.48 ± 0.87	3.32 ± 0.87*	0.004

Values are mean ± S.D. or percentages. Hypertension was defined as a systolic blood pressure of 140 mm Hg or higher, a diastolic blood pressure of 90 mm Hg or higher, or current use of antihypertensive drugs. Diabetes mellitus was defined as a non-fasting blood glucose of 11.1 mmol/L (200 mg/dL) or higher, or the current use of diabetic drugs or insulin infusion.

* $P < 0.05$ compared with B1B1.

\# $P < 0.05$ compared with B1B2.

Table 2
Multivariate linear regression analysis of determinants for HDL cholesterol levels in 1999, Shiga, Japan

	Dependent variable	Independent variables	Men ($N=659$)		Women ($N=1070$)	
			β	p-value	β	p-value
Model 1	HDL-C (mmol/L)	Age (10-year)	−0.010 (0.008)	0.208	0.040 (0.008)	<0.001
		Waist to hip ratio	−0.706 (0.203)	<0.001	−0.987 (0.202)	<0.001
		Alcohol drinking				
		Non-drinker	Reference		Reference	
		Drinker	0.142 ((0.027))	<0.001	0.047 (0.023)	0.040
		Current smoking				
		Non-smoker	Reference		Reference	
		Smoker	−0.054 (0.024)	0.026	−0.019 (0.042)	0.658
		Non-HDL cholesterol (mmol/L)	0.023 (0.017)	0.165	0.015 (0.014)	0.280
		Triglyceride (log-transferred, mmol/L)	−0.678 (0.061)	<0.001	−0.703 (0.055)	< 0.001
		CETP *Taq*IB genotype				
		B1B1 or B1B2	Reference		Reference	
		B2B2	0.065 (0.033)	0.049	0.118 (0.028)	< 0.001
Model 2	HDL-C (mmol/L)	Age (10-year)	−0.010 (0.008)	0.215	0.039 (0.008)	<0.001
		Waist to hip ratio	−0.703 (0.204)	<0.001	−0.963 (0.202)	<0.001
		Alcohol drinking				
		Non-drinker	Reference		Reference	
		Drinker	0.141 (0.027)	<0.001	0.046 (0.023)	0.047
		Current smoking				
		Non-smoker	Reference		Reference	
		Smoker	−0.053 (0.024)	0.031	−0.020 (0.042)	0.639
		Non-HDL cholesterol (mmol/L)	0.023 (0.017)	0.160	0.014 (0.014)	0.310
		Triglyceride (log-transferred, mmol/L)	−0.678 (0.061)	<0.001	−0.697 (0.055)	<0.001
		CETP *Taq*IB genotype				
		B1B1 or B1B2	Reference		Reference	
		B2B2	0.068 (0.034)	0.046	0.114 (0.028)	<0.001
		CETP *Taq*IB genotype × Waist to hip ratio	0.179 (0.503)	0.721	0.300 (0.467)	0.522
		CETP *Taq*IB genotype × Alcohol drinking	−0.041 (0.078)	0.597	0.156 (0.062)	0.012
		CETP *Taq*IB genotype × Current smoking	0.014 (0.071)	0.842	−0.052 (0.118)	0.659

β indicates regression coefficient (SE). Status of alcohol drinking or current smoking is coded as 0, 1. CETP *Taq*IB genotype is coded as follows; B1B1 or B1B2, 0; B2B2, 1.

W/H ratio ($r=0.66$, $p<0.001$ in men, $r=0.62$, $p<0.001$ in women), we used W/H ratio, which had a stronger association to HDL cholesterol levels than BMI. Model 2 was performed with the same covariates as model 1 but included interaction between the *Taq*IB genotype and W/H ratio, alcohol drinking, or current smoking. In the analysis using model 1, W/H ratio, alcohol drinking, current smoking habit, logarithm of TG, and the CETP *Taq*IB genotype were the determinants of HDL cholesterol levels in men. Meanwhile, the determinants of HDL cholesterol levels in women were the same as those in men except for age and current smoking. In the analysis using model 2, interaction between the CETP *Taq*IB genotype and alcohol drinking was observed in women.

Fig. 1 describes the relationship between the CETP *Taq*IB polymorphism and HDL cholesterol levels stratified by alcohol consumption. Among men who consumed less than 2 drinks/day, the mean HDL cholesterol levels were not significantly different among the three *Taq*IB genotypes (B1B1, 1.31 ± 0.03; B1B2, 1.28 ± 0.02; B2B2, 1.33 ± 0.05 mmol/L, mean ± S.E., $p=0.586$). However, among men who consumed 2 or more drinks/day, the mean HDL cholesterol levels were higher among those with the B2B2 genotype than those with the B1B1 genotype (B1B1, 1.37 ± 0.03; B1B2, 1.44 ± 0.03; B2B2, 1.49 ± 0.05 mmol/L, $p=0.042$). The interaction between alcohol consumption and the CETP *Taq*IB polymorphism to the HDL cholesterol levels was not significant ($p=0.165$). However, when the CETP *Taq*IB genotypes were divided into two groups, the B1B1 genotype and the B1B2 + B2B2 genotypes, the interaction between alcohol consumption and the CETP *Taq*IB polymorphism to the HDL cholesterol levels were significant ($p'=0.049$). Among women who did not drink, the mean HDL cholesterol levels were lower among those with the B1B1 genotype than those with the other genotypes (B1B1, 1.51 ± 0.02; B1B2, 1.58 ± 0.02; B2B2, 1.63 ± 0.03 mmol/L, $p<0.001$). Among women who consumed alcohol, the mean HDL cholesterol levels were higher among those with the B2B2 genotype than those with the other genotypes (B1B1, 1.57 ± 0.03;

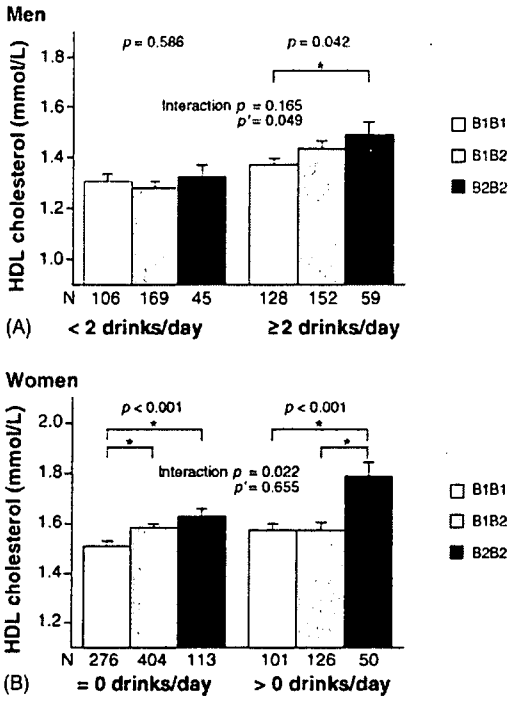

Fig. 1. Adjusted HDL cholesterol levels according to alcohol consumption and the CETP *Taq*IB genotype in the participants in men (A) and women (B). HDL cholesterol levels were adjusted for confounding factors: age, W/H ratio, current smoking status, non-HDL cholesterol, and logarithm of triglycerides. Since the average levels of alcohol consumption were much lower among women than men, alcohol consumption was categorized as more than 2 drinks/day for men and any alcohol consumption for women. To compare mean values among the three genotypes within the lower alcohol consumption group or higher alcohol consumption group, one-way ANOVA was used. To assess the interaction between alcohol consumption and the CETP *Taq*IB polymorphism in the regulation of HDL cholesterol levels, ANCOVA was used. p-value were calculated among the participants with three genotypes. p'-values were calculated between the participants with the B1B1 genotype and the B1B2 + B2B2 genotypes. All values are mean ± S.E. $^{*}p < 0.05$.

B1B2, 1.57 ± 0.03; B2B2, 1.79 ± 0.06 mmol/L, $p < 0.001$). The interaction between alcohol consumption and the CETP *Taq*IB polymorphism to the HDL cholesterol levels was significant ($p = 0.022$).

We also examined the interaction between the CETP *Taq*IB polymorphism and current smoking status, BMI, or W/H ratio in the regulation of HDL cholesterol levels. However, no significant interactions were observed (data not shown).

4. Discussion

In the present study, we studied the association between the CETP *Taq*IB polymorphism and the HDL cholesterol levels considering environmental factors in a population-based sample consisting of 1729 Japanese men and women. Our results showed that the B2 allele was associated with higher HDL cholesterol levels in women and the CETP *Taq*IB polymorphism was an independent determinant of HDL cholesterol levels in men and women. We compared the HDL cholesterol levels according to the CETP *Taq*IB genotype stratified by alcohol consumption, current smoking status, BMI, or W/H ratio. The correlation of the B2 allele with increased HDL cholesterol levels was stronger in alcohol consumers than that observed with non-drinkers in men and women.

In the present study, the effect of the B2 allele to increase HDL cholesterol levels was stronger in women than men. This is consistent with the result in the meta-analysis of the CETP *Taq*IB polymorphism [20]. Previous studies showed that the effect of the B2 allele to increase HDL cholesterol level was stronger in alcohol consumers [11,21], nonsmokers [5,7,8], and lean participants [8]. However, no significant interactions were reported between the CETP *Taq*IB polymorphism and smoking, alcohol drinking, or daily physical activity in the regulation of HDL cholesterol in the Japanese general population [22]. In the present study, the interaction between alcohol consumption and the CETP *Taq*IB polymorphism in the regulation of HDL cholesterol was significant in men and women. This result is consistent with previous results [11,21] in Caucasian populations. However, the interaction was found to be only suggestive in the meta-analysis [20]. Most studies included in the meta-analysis did not record alcohol consumption in a detailed manner, the information of alcohol consumption was only divided as drinkers and non-drinkers in the meta-analysis, which may have attenuated the power to detect such an interaction. In the present study we analyzed men and women separately because average HDL cholesterol levels were different between men and women (men, 1.36 ± 0.01; women, 1.58 ± 0.01 mmol/l, mean ± S.E., $p < 0.001$). Moreover, since the average levels of alcohol consumption were much lower among women than men (men, 21.1 ± 0.8; women, 2.9 ± 0.2 g/day, mean ± SE, $p < 0.001$), alcohol consumption was categorized as more than 2 drinks/day for men and any alcohol consumption for women. These procedures may keep the power to detect the interaction in the present study.

HDL cholesterol level is known to increase with alcohol consumption at least in part due to reduced concentration and activity of plasma CETP [23]. The expected association between alcohol consumption and plasma HDL cholesterol was clearly observed in the B2 homozygotes but not in the B1 homozygotes in the present study. The CETP *Taq*IB polymorphism was reported to be in strong linkage disequilibrium with the −629 C to A promoter polymorphism [21]. This promoter polymorphism modulates CETP gene transcriptional activity in vitro [24]. Recently, −1337 C/T and −971 G/A polymorphisms in the CETP promoter were also reported to be functional and these three polymorphisms interact together to determine plasma CETP levels [25]. The mechanisms of the interaction between the CETP *Taq*IB polymorphism and alcohol consumption in the regulation of plasma HDL choles-

terol are unclear. It may be possible that these promoter polymorphisms play a part in the mechanisms of the interaction.

The effect of the B2 allele to increase HDL cholesterol levels has been reported to be stronger in non-smokers [5,7,8]. In the present study, the interaction between current smoking status and the CETP *Taq*IB polymorphism was not observed in men or women. Several studies have also reported no evidence of an interaction with smoking status [11,22].

The association of the B2 allele with increased HDL cholesterol levels has been reported in lean participants, but not in obese participants [8]. In the present study, we used the W/H ratio instead of BMI. The interaction between W/H ratio and the CETP *Taq*IB polymorphism was not observed either in men or women. When we performed an analysis using BMI, results similar to those using W/H ratio were obtained. The average BMI in Japanese is lower than the average Caucasian BMI (mean BMI was 25.0 kg/m^2 for a Caucasian population [8], versus 22.5 kg/m^2 in this study). Thus, the different result may be due to differing mean BMI.

The effect of the B2 allele to increase HDL cholesterol levels has been reported to be weaker in the postmenopausal than that in premenopausal women [10]. We did not have any menopausal information in the present study. Instead of the menopausal information, we considered menopause effects by grouping the women participants by age: ≥55 years old or <55 years old. However, no effects were observed for the relationship among the CETP *Taq*IB polymorphism, HDL cholesterol levels, and other variables (data not shown).

There are some limitations in the present study. First, we did not examine other mutations in the CETP locus. Several mutations at the CETP locus have been identified, resulting in the total or partial absence of detectable CETP mass and/or activity [26,27] and increased HDL cholesterol levels. G to A mutation at the intron 14 splice donor site (Int14 A) and a missense mutation within exon 15 (D442G) are common in the Japanese population [28]. We also did not consider physical activity of participants in the present study, which is known to affect HDL cholesterol levels [29]. Moreover, we used non-fasting blood samples in the present study, thus TG levels were influenced by diet. However, non-fasting TG is reported to be an independent risk factor for CHD in the Japanese general population [30]; therefore, we used non-fasting TG values as a co-factor in the present study. The prevalence of smoking was significantly lower in the participants with the B2B2 genotype in men. We have no possible explanation for this and it may have been a confounder. The mean values of non-HDL cholesterol were significantly lower in the participants with the B2B2 genotype than the B1B1 genotype in women. This may be because the mean values of age were significantly lower in the participants with the B2B2 genotype than the B1B1 genotype in women. The interaction between smoking and the CETP genotype in determining HDL cholesterol levels was absent in both men and women. However, the rate of smoking was very low in women; therefore, this study has no power to detect the interaction between smoking and the CETP genotype in determining HDL cholesterol levels in women.

In conclusion, there is a gene-environmental interaction between the CETP *Taq*IB polymorphism and alcohol consumption in the regulation of HDL cholesterol levels in men and women.

Acknowledgments

This study was supported by a Grant-in-Aid for Scientific Research (C:16590500) from the Japan Society for Promotion of Science and a Grant-in-Aid for Scientific Research on Priority Areas (1601227) from the Japanese Ministry of Education, Culture, Sports, Science and Technology.

References

[1] Rhoads GG, Gulbrandsen CL, Kagan A. Serum lipoproteins and coronary heart disease in a population study of Hawaii Japanese men. N Engl J Med 1976;294:293–8.
[2] Okamura T, et al. The inverse relationship between serum high-density lipoprotein cholesterol level and all-cause mortality in a 9.6-year follow-up study in the Japanese general population. Atherosclerosis 2006;184:143–50.
[3] Yen FT, Deckelbaum RJ, Mann CJ, et al. Inhibition of cholesteryl ester transfer protein activity by monoclonal antibody. Effects on cholesteryl ester formation and neutral lipid mass transfer in human plasma. J Clin Invest 1989;83:2018–24.
[4] Drayna D, Lawn R. Multiple RFLPs at the human cholesteryl ester transfer protein (CETP) locus. Nucleic Acids Res 1987;15:4698.
[5] Hannuksela ML, Liinamaa MJ, Kesaniemi YA, Savolainen MJ. Relation of polymorphisms in the cholesteryl ester transfer protein gene to transfer protein activity and plasma lipoprotein levels in alcohol drinkers. Atherosclerosis 1994;110:35–44.
[6] Kuivenhoven JA, de Knijff P, Boer JM, et al. Heterogeneity at the CETP gene locus. Influence on plasma CETP concentrations and HDL cholesterol levels. Arterioscler Thromb Vasc Biol 1997;17:560–8.
[7] Kondo I, Berg K, Drayna D, Lawn R. DNA polymorphism at the locus for human cholesteryl ester transfer protein (CETP) is associated with high density lipoprotein cholesterol and apolipoprotein levels. Clin Genet 1989;35:49–56.
[8] Freeman DJ, Griffin BA, Holmes AP, et al. Regulation of plasma HDL cholesterol and subfraction distribution by genetic and environmental factors. Associations between the TaqI B RFLP in the CETP gene and smoking and obesity. Arterioscler Thromb 1994;14:336–44.
[9] Mitchell RJ, Earl L, Williams J, Bisucci T, Gasiamis H. Polymorphisms of the gene coding for the cholesteryl ester transfer protein and plasma lipid levels in Italian and Greek migrants to Australia. Hum Biol 1994;66:13–25.
[10] Kauma H, Savolainen MJ, Heikkila R, et al. Sex difference in the regulation of plasma high density lipoprotein cholesterol by genetic and environmental factors. Hum Genet 1996;97:156–62.
[11] Fumeron F, Betoulle D, Luc G, et al. Alcohol intake modulates the effect of a polymorphism of the cholesteryl ester transfer protein gene on plasma high density lipoprotein and the risk of myocardial infarction. J Clin Invest 1995;96:1664–71.
[12] Choudhury SR, Ueshima H, Kita Y, et al. Alcohol intake and serum lipids in a Japanese population. Int J Epidemiol 1994;23:940–7.

[13] Kuivenhoven JA, et al. The role of a common variant of the cholesteryl ester transfer protein gene in the progression of coronary atherosclerosis. N Engl J Med 1998;338:86–93.
[14] Gordon DJ, Rifkind BM. High-density lipoprotein–the clinical implications of recent studies. N Engl J Med 1989;321:1311–6.
[15] Stamler J, Elliott P, Appel L, et al. Higher blood pressure in middle-aged American adults with less education-role of multiple dietary factors: the INTERMAP study. J Hum Hypertens 2003;17:655–775.
[16] Nakamura Y, Amamoto K, Tamaki S, et al. Genetic variation in aldehyde dehydrogenase 2 and the effect of alcohol consumption on cholesterol levels. Atherosclerosis 2002;164:171–7.
[17] Tamaki S, Nakamura Y, Tsujita Y, et al. Polymorphism of the angiotensin converting enzyme gene and blood pressure in a Japanese general population (the Shigaraki Study). Hypertens Res 2002;25:843–8.
[18] Amamoto K, Okamura T, Tamaki S, et al. Epidemiologic study of the association of low-Km mitochondrial acetaldehyde dehydrogenase genotypes with blood pressure level and the prevalence of hypertension in a general population. Hypertens Res 2002;25:857–64.
[19] Myers GL, Cooper GR, Henderson LO, Hassemer DJ, Kimberly MM. Standardization of lipid and lipoprotein measurement. In: Rifai N, Warnick GR, Dominiczak MH, editors. Handbook of lipoprotein testing. Washington, DC: AACC; 1997. p. 223–50.
[20] Boekholdt SM, Sacks FM, Jukema JW, et al. Cholesteryl ester transfer protein TaqIB variant, high-density lipoprotein cholesterol levels, cardiovascular risk, and efficacy of pravastatin treatment: individual patient meta-analysis of 13,677 subjects. Circulation 2005;111:278–87.
[21] Corbex M, Poirier O, Fumeron F, et al. Extensive association analysis between the CETP gene and coronary heart disease phenotypes reveals several putative functional polymorphisms and gene-environment interaction. Genet Epidemiol 2000;19:64–80.
[22] Chen J, Yokoyama T, Saito K, et al. Association of human cholesteryl ester transfer protein-TaqI polymorphisms with serum HDL cholesterol levels in a normolipemic Japanese rural population. J Epidemiol 2002;12:77–84.
[23] Hannuksela M, Marcel YL, Kesaniemi YA, Savolainen MJ. Reduction in the concentration and activity of plasma cholesteryl ester transfer protein by alcohol. J Lipid Res 1992;33:737–44.
[24] Dachet C, Poirier O, Cambien F, Chapman J, Rouis M. New functional promoter polymorphism, CETP/-629, in cholesteryl ester transfer protein (CETP) gene related to CETP mass and high density lipoprotein cholesterol levels: role of Sp1/Sp3 in transcriptional regulation. Arterioscler Thromb Vasc Biol 2000;20:507–15.
[25] Frisdal E, Klerkx AH, Le Goff W, et al. Functional interaction between −629C/A, −971G/A and −1337C/T polymorphisms in the CETP gene is a major determinant of promoter activity and plasma CETP concentration in the REGRESS Study. Hum Mol Genet 2005;14:2607–18.
[26] Brown ML, Inazu A, Hesler CB, et al. Molecular basis of lipid transfer protein deficiency in a family with increased high-density lipoproteins. Nature 1989;342:448–51.
[27] Takahashi K, Jiang XC, Sakai N, et al. A missense mutation in the cholesteryl ester transfer protein gene with possible dominant effects on plasma high density lipoproteins. J Clin Invest 1993;92:2060–4.
[28] Inazu A, Jiang XC, Haraki T, et al. Genetic cholesteryl ester transfer protein deficiency caused by two prevalent mutations as a major determinant of increased levels of high density lipoprotein cholesterol. J Clin Invest 1994;94:1872–82.
[29] Ordovas JM. HDL genetics: candidate genes, genome wide scans and gene-environment interactions. Cardiovasc Drugs Ther 2002;16:273–81.
[30] Iso H, Naito Y, Sato S, et al. Serum triglycerides and risk of coronary heart disease among Japanese men and women. Am J Epidemiol 2001;153:490–9.

British Journal of Pharmacology (2007) 150, 1011–1021

0007–1188/07 $30.00
www.brjpharmacol.org

RESEARCH PAPER

Stimulatory action of protein kinase Cε isoform on the slow component of delayed rectifier K^+ current in guinea-pig atrial myocytes

H Toda[1,2], W-G Ding[1], Y Yasuda[1,2], F Toyoda[1], M Ito[2], H Matsuura[1] and M Horie[2]

[1]*Department of Physiology, Shiga University of Medical Science, Otsu, Shiga, Japan and* [2]*Department of Cardiovascular and Respiratory Medicine, Shiga University of Medical Science, Otsu, Shiga, Japan*

Background and purpose: Protein kinase C (PKC) comprises at least twelve isoforms and has an isoform-specific action on cardiac electrical activity. The slow component of delayed rectifier K^+ current (I_{Ks}) is one of the major repolarizing currents in the hearts of many species and is also potentiated by PKC activation. Little is known, however, about PKC isoform(s) functionally involved in the potentiation of I_{Ks} in native cardiac myocytes.
Experimental approach: I_{Ks} was recorded from guinea-pig atrial myocytes, using the whole-cell configuration of patch-clamp method.
Key results: Bath application of phenylephrine enhanced I_{Ks} concentration-dependently with EC_{50} of 5.4 μM and the maximal response (97.1 ± 11.9% increase, $n = 16$) was obtained at 30 μM. Prazosin (1 μM) almost totally abolished the potentiation of I_{Ks} by phenylephrine, supporting the involvement of α_1-adrenoceptors. The stimulatory action of phenylephrine was significantly, if not entirely, inhibited by the general PKC inhibitor bisindolylmaleimide I but was little affected by Gö-6976, Gö-6983 and rottlerin. Furthermore, this stimulatory effect was significantly reduced by dialyzing atrial myocytes with PKCε-selective inhibitory peptide εV1-2 but was not significantly affected by conventional PKC isoform-selective inhibitory peptide βC2-4. Phorbol 12-myristate 13-acetate (PMA) at 100 nM substantially increased I_{Ks} by 64.2 ± 1.3% ($n = 6$), which was also significantly attenuated by an internal dialysis with εV1-2 but not with βC2-4.
Conclusions and implications: The present study provides experimental evidence to suggest that, in native guinea-pig cardiac myocytes, activation of PKC contributes to α_1-adrenoceptor-mediated potentiation of I_{Ks} and that ε is the isoform predominantly involved in this PKC action.
British Journal of Pharmacology (2007) **150**, 1011–1021. doi:10.1038/sj.bjp.0707191; published online 5 March 2007

Keywords: I_{Ks}; PKC; PKCε; phenylephrine; α_1-adrenoceptor

Abbreviations: BIS-I, bisindolylmaleimide I; DAG, diacylglycerol; $I_{Ca,L}$, L-type Ca^{2+} inward current; I_K, delayed rectifier K^+ current; I_{Kr}, rapid component of delayed rectifier K^+ current; I_{Ks}, slow component of delayed rectifier K^+ current; PDBu, phorbol 12,13-dibutyrate; PKA, cyclic AMP-dependent protein kinase; PKC, protein kinase C; PLC, phospholipase C; PMA, phorbol 12-myristate 13-acetate; PS, phosphatidylserine; PtdIns(4,5)P_2, phosphatidylinositol 4,5-bisphosphate; RACKs, receptors for activated C kinases; TPA, 12-*O*-tetradecanoylphorbol 13-acetate

Introduction

Protein kinase C (PKC) mediates the regulation of cardiac muscle function by a variety of neurotransmitters, hormones and extracellular signalling molecules. Currently, at least 12 isoforms of PKC have been identified in various tissues and are classified into three groups based on their structure and activation mechanisms (Mellor and Parker, 1998); namely, conventional PKC (α, βI, βII and γ) that have a C2-domain and are activated by Ca^{2+}, diacylglycerol (DAG) and phosphatidylserine (PS); novel PKC (δ, ε, μ, θ and η) that do not have a C2-domain and are activated by DAG and PS; and atypical PKC (ζ and λ) that are regulated by PS. Expression of PKC isoforms in the heart displays species- and/or developmental stage-dependent differences (Pucéat *et al.*, 1994; Rybin and Steinberg, 1994). It has been demonstrated that guinea-pig heart coexpresses conventional (α, βII and γ), novel (ε) and atypical (ζ) PKC isoforms (Takeishi *et al.*, 1999). There is accumulating evidence to indicate that PKC isoforms in the heart are differentially regulated by various

Correspondence: Dr H Matsuura, Department of Physiology, Shiga University of Medical Science, Otsu, Shiga 520-2192, Japan.
E-mail: matuurah@belle.shiga-med.ac.jp
Received 21 September 2006; revised 13 December 2006; accepted 16 January 2007; published online 5 March 2007

stimuli under physiological and pathological conditions (Takeishi *et al.*, 1999; Hool, 2000; Ruf *et al.*, 2002) and have different functional roles in the modulation of electrical activity (Johnson and Mochly-Rosen, 1995) and the development of cardiac hypertrophy and heart failure (Bowling *et al.*, 1999; Takeishi *et al.*, 2000). In this regard, it is important to note that PKCε has been shown to contribute to cardiac protection associated with ischemic preconditioning (Gray *et al.*, 1997; Qiu *et al.*, 1998; Liu *et al.*, 1999).

The slow component of the delayed rectifier K^+ current (I_{Ks}) is important for the repolarization of atrial (Sanguinetti and Jurkiewicz, 1991; Wang *et al.*, 1993; Gintant, 1996; Bosch *et al.*, 2003; Ding *et al.*, 2004) and ventricular action potentials (Sanguinetti and Jurkiewicz, 1990; Li *et al.*, 1996; Bosch *et al.*, 1998) in the heart of several mammalian species including humans. I_{Ks} also represents a relevant target for the action of the sympathetic neurotransmitters, adrenaline and noradrenaline, and thereby mediates sympathetic control of cardiac excitability and contractility (Sanguinetti *et al.*, 1991). Stimulation of β-adrenoceptors has been shown to markedly enhance I_{Ks} via activation of the cyclic AMP-dependent protein kinase (PKA) in some types of myocardial cells, including atrial and ventricular myocytes (Walsh and Kass, 1988; Yazawa and Kameyama, 1990; Matsuura *et al.*, 1996). On the other hand, it has been demonstrated in guinea-pig ventricular myocytes that α_1-adrenoceptor stimulation produced a modest (approximately 20–30%) increase in I_{Ks} via activation of PKC (Tohse *et al.*, 1992). The elevated sympathetic tone is accompanied by an enhancement of outward K^+ current through I_{Ks}, which is assumed to counteract the depolarizing effect of the simultaneously potentiated L-type Ca^{2+} inward current ($I_{Ca,L}$) and thereby prevents the excess prolongation of action potential duration, potentially leading to the occurrence of arrhythmias as well as Ca^{2+} overload in cardiac muscle. Thus, the stimulatory action of both α_1- and β-adrenoceptors on I_{Ks} appears to play an important physiological role in protecting the heart from the arrhythmogenic and cardiotoxic effects of excess sympathetic activity.

The present study was undertaken to determine which PKC isoform(s) is functionally involved in mediating the stimulatory action of α_1-adrenoceptor activation, as well as PMA, on I_{Ks}, with the use of the PKC isoform-selective inhibitory peptides and pharmacological inhibitors. Our results provide experimental evidence supporting a functional role of ε isoform of PKC (PKCε) in mediating α_1-adrenergic potentiation of I_{Ks} in native atrial myocytes of guinea-pig hearts.

Materials and methods

Isolation of atrial myocytes

All animal procedures were performed in accordance with the guidelines established by the institution's Animal Care and Use Committee. Single atrial myocytes were enzymatically isolated from adult Hartley guinea-pig hearts using a retrograde Langendorff perfusion method as described previously (Powell *et al.*, 1980; Ding *et al.*, 2004).

Solutions and chemicals

Normal Tyrode solution contained (in mM) 140 NaCl, 5.4 KCl, 1.8 $CaCl_2$, 0.5 $MgCl_2$, 0.33 NaH_2PO_4, 5.5 glucose and 5.0 HEPES (pH adjusted to 7.4 with NaOH). The extracellular bath solution used for measuring I_{Ks} was normal Tyrode solution supplemented with 0.4 μM nisoldipine (a generous gift from Bayer AG, Wuppertal-Elberfeld, Germany) and 5 μM E-4031 (Wako, Osaka, Japan). Agents added to the extracellular solution included phenylephrine hydrochloride (Sigma, St Louis, MO, USA), prazosin hydrochloride (Sigma), phorbol 12-myristate 13-acetate (PMA, Sigma), bisindolylmaleimide I (BIS-I, Sigma), Gö-6976 (Calbiochem, San Diego, CA, USA), Gö-6983 (Biomol, Plymouth Meeting, PA, USA), rottlerin (Calbiochem) and thymeleatoxin (Calbiochem). The control pipette solution contained (in mM) 70 potassium aspartate, 50 KCl, 10 KH_2PO_4, 1 $MgSO_4$, 3 Na_2-ATP (Sigma), 0.1 Li_2-GTP (Roche Diagnostics GmbH, Mannheim, Germany), 5 EGTA, 0.5 $CaCl_2$ and 5 HEPES (pH adjusted to 7.2 with KOH). The concentration of free Ca^{2-} and Mg^{2-} in the pipette solution was calculated to be approximately 1.7×10^{-8} (pCa = 7.8) and 3.7×10^{-5} M (pMg = 4.4), respectively (Fabiato and Fabiato, 1979; Tsien and Rink, 1980). It should be noted that conventional PKC isoforms can be functionally activated by the presence of intracellular free Ca^{2+} concentration on the order of 10^{-8} M in guinea-pig cardiac myocytes (Hool, 2000). In some experiments, peptide translocation inhibitor of PKC isoform βC2-4 or εV1-2 (Biomol) was added to the pipette solution and was present throughout the recording period (Ron *et al.*, 1995; Johnson *et al.*, 1996).

Whole-cell patch-clamp technique and data analysis

Whole-cell membrane currents (Hamill *et al.*, 1981) were recorded with an EPC-8 patch-clamp amplifier (HEKA, Lambrecht, Germany), and data were low-pass filtered at 1 kHz, acquired at 5 kHz through an LIH-1600 analog-to-digital converter (HEKA) and stored on hard disc drive, using PATCHMASTER software (HEKA). Patch electrodes had a resistance of 1.8–2.5 MΩ when filled with pipette solutions, and approximately 10 min was allowed to elapse to dialyze the interior of cells with test reagents (βC2-4 or εV1-2) in pipette solution. Cells were superfused constantly at 1–2 ml min^{-1} with extracellular solution at 36 ± 1 C in a 0.5 ml bath chamber.

I_{Ks} was activated by depolarizing voltage steps given from a holding potential of −50 mV to various levels, under conditions where the Na^+ current was inactivated by setting the holding potential to −50 mV, and $I_{Ca,L}$ and the rapid component of delayed rectifier K^+ current (I_{Kr}) were, respectively, blocked by nisoldipine (0.4 μM) and E-4031 (5 μM) added to the extracellular solution for the measurement of I_{Ks} (Ding *et al.*, 2004). The effect of external application of test reagents on I_{Ks} was investigated after the initial rundown of I_{Ks} within 3–5 min of patch rupture was allowed to reach a steady-state level, and the initial rundown of I_{Ks} is not shown in the figures. The period of exposure to various reagents is denoted by the horizontal bar in the figures, and the original current traces recorded at time points indicated by numerals are also illustrated in the inset.

The zero-current level is indicated to the left of current traces by the horizontal line.

Voltage-dependent activation of I_{Ks} was assessed by fitting the normalized *I–V* relationship of the tail currents to a Boltzmann equation: $I_{Ks,tail} = 1/(1+\exp((V_{1/2}-V_m)/k))$, where $I_{Ks,tail}$ is the tail current amplitude normalized with reference to the maximum value measured at +50 mV, $V_{1/2}$ is the voltage at half-maximal activation, V_m is the test potential and k is the slope factor. Concentration–response relationship for the potentiation of I_{Ks} by phenylephrine was drawn by least-squares fit of a Hill equation: $R = R_{max}/(1+(EC_{50}/[agonist])^{nH})$, where R_{max} represents the maximal degree of potentiation expressed as a percentage, EC_{50} is the concentration giving half-maximal potentiation and n_H is the Hill coefficient.

Statistical analysis

All the averaged data are presented as mean±s.e.m. with the number of experiments given in parentheses. Statistical comparisons were evaluated using either Student's *t*-test or analysis of variance (ANOVA) with Student–Newman–Keuls (SNK) *post hoc* analysis, as appropriate. Differences were considered to be statistically significant if a *P*-value <0.05 was obtained.

Results

Potentiation of I_{Ks} by phenylephrine via α_1-adrenoceptor in guinea-pig atrial myocytes

We first characterized the stimulatory action of phenylephrine on I_{Ks} in guinea-pig atrial myocytes. Figure 1a demonstrates a representative example for the time course of I_{Ks} response to 30 μM phenylephrine. I_{Ks} was repetitively (once every 20 s) activated by depolarizing voltage steps (2 s in duration) applied from a holding potential of −50 mV to a test potential of +30 mV, and the effect of phenylephrine on I_{Ks} was evaluated by measuring the amplitude of the tail current elicited upon return to the holding potential, which reflects the degree of I_{Ks} activation at the preceding depolarizing test potential. In a total of 16 myocytes, bath application of 30 μM phenylephrine evoked a marked (97.1±11.9%) increase in the amplitude of I_{Ks} in a reversible manner (see also Figures 2d and 4).

Figure 1b shows superimposed current traces of I_{Ks} elicited by depolarizing voltage steps given from a holding potential of −50 mV to various test potentials between −40 and +50 mV, before and during exposure to 30 μM phenylephrine. As is evident in Figure 1c, phenylephrine markedly increased the amplitude of I_{Ks} tail currents at all test potentials. To elucidate whether phenylephrine affects the voltage dependence of I_{Ks} activation, the amplitude of tail current at each test potential was normalized with reference to its maximal value at +50 mV and was then fitted by a Boltzmann equation (Figure 1d). The data points were reasonably well fitted by a Boltzmann equation, yielding $V_{1/2}$ of 8.6±2.4 mV and k of 12.7±0.7 mV for control, and $V_{1/2}$ of 5.0±3.2 mV and k of 12.9±0.7 mV for phenylephrine ($n=4$). There were no significant differences in the values of $V_{1/2}$ ($P=0.133$) and k ($P=0.850$) between control and phenylephrine groups, thus suggesting that phenylephrine has little effect on the voltage dependence of current activation.

In the experiments demonstrated in Figure 2a, the effect of phenylephrine on I_{Ks} was examined in the presence of the selective α_1-adrenoceptor antagonist prazosin. The atrial myocytes were initially exposed to 1 μM prazosin for ~5 min, and then to 30 μM phenylephrine in the presence of prazosin. The stimulatory action of phenylephrine on I_{Ks} was almost totally abolished by the presence of prazosin (3.7±3.3% increase, $n=6$ versus 97.1±11.9% increase, $n=16$; Figure 2b). It should be noted that the amplitude of I_{Ks} was only slightly decreased (by 5.3±2.5%, $n=6$) during exposure to 1 μM prazosin alone (Figure 2a). This observation confirms the view that the action of phenylephrine on I_{Ks} is mediated through the α_1-adrenoceptor. The potentiation of I_{Ks} by phenylephrine was examined at concentrations ranging from 0.3 to 100 μM. Figure 2c illustrates representative examples for the effect of 1 and 100 μM phenylephrine (left and right panels, respectively). Figure 2d depicts the concentration–response relationship for the stimulatory action of phenylephrine on I_{Ks}, which could be reasonably well fitted with a Hill equation with EC_{50} of 5.4 μM and n_H of 1.03.

We also evaluated the effect of phenylephrine (30 μM) on the time course of I_{Ks} activation during depolarizations in the absence and presence of prazosin. For this purpose, the time to obtain half-maximal activation ($T_{1/2}$, Stengl *et al.*, 2003; Terrenoire *et al.*, 2005) during 2-s depolarizing voltage steps was compared before and during exposure to phenylephrine. In the absence of prazosin (refer to experiments shown in Figure 1b), $T_{1/2}$ at test potentials of +10, +30 and +50 mV were, respectively, measured to be 484±56, 342±40 and 305±33 ms ($n=5$) before phenylephrine and 432±26, 346±34 and 307±44 ms during exposure to phenylephrine. There were no significant differences in the value of $T_{1/2}$ obtained at each test potential (+10, +30 or +50 mV) before and during exposure to phenylephrine. Similarly, in the presence of 1 μM prazosin (refer to experiments shown in Figure 2a), $T_{1/2}$ at a test potential of +30 mV (322±10 ms, $n=5$) was insignificantly affected by further addition of phenylephrine (317±8 ms). These observations are in contrast to an increase in the rate of channel activation during β-adrenergic potentiation of I_{Ks} (Han *et al.*, 2001; Stengl *et al.*, 2003; Volders *et al.*, 2003; Terrenoire *et al.*, 2005). Taken together with the results using prazosin (Figure 2b), these data also support a predominant role of α_1-adrenoceptors in potentiation of I_{Ks} by phenylephrine.

Functional role of novel PKC isoform PKCε in potentiation of I_{Ks} by phenylephrine

We then evaluated a role for PKC and its isoforms in the potentiation of I_{Ks} via α_1-adrenoceptors. For this purpose, the stimulatory action of phenylephrine was measured at its maximally effective concentration (30 μM, Figure 2d) in the presence of various pharmacological (bath) and peptide inhibitors (pipette) for PKC isoforms. Figure 3a illustrates a

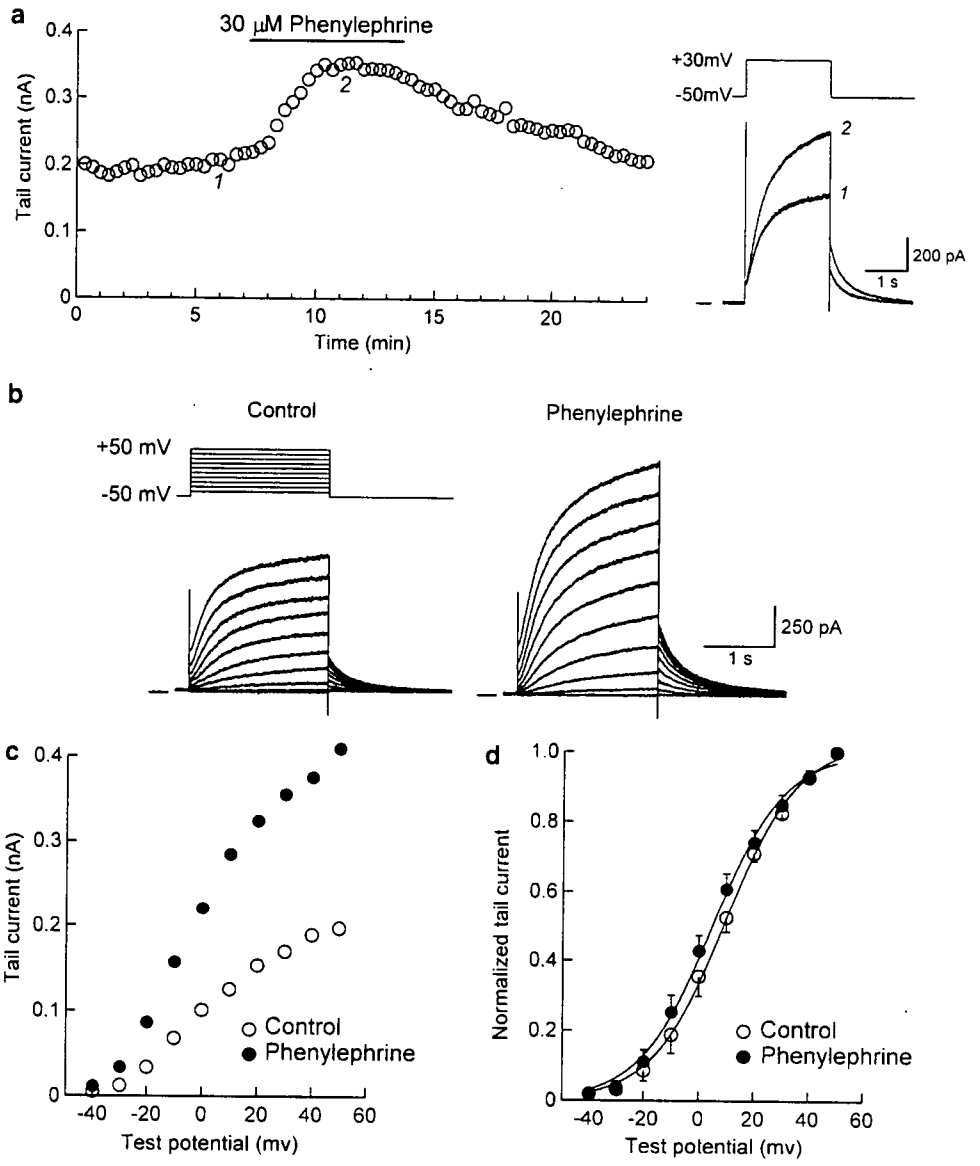

Figure 1 Potentiation of I_{Ks} by phenylephrine in guinea-pig atrial myocytes. (**a**) Time course of changes in the amplitude of I_{Ks} tail current during exposure to 30 μM phenylephrine. I_{Ks} was repetitively (every 20 s) activated by 2-s depolarizing steps to + 30 mV from a holding potential of −50 mV. (**b**) Superimposed current traces of I_{Ks} activated at test potentials of −40 to + 50 mV, before and ~5 min after exposure to 30 μM phenylephrine. **a** and **b** were obtained from different myocytes. (**c**) *I–V* relationships for I_{Ks} tail currents recorded before and during exposure to phenylephrine, obtained from the records in **b**. (**d**) *I–V* relationships for mean values ($n=4$) of normalized I_{Ks} tail currents. Continuous curves through the data points show the least-squares fit of a Boltzmann equation.

typical example for the action of the general (nonisoform-specific) PKC inhibitor BIS-I (Toullec *et al.*, 1991), which at submicromolar concentrations potently inhibits most PKC isoforms, including conventional (α, βI, βII and γ), novel (δ and ε) and atypical (ζ) isoforms (Martiny-Baron *et al.*, 1993). In a total of six myocytes, phenylephrine (30 μM) potentiated the amplitude of I_{Ks} by 38.1 ± 12.1% in the presence of BIS-I (100 nM), which is significantly smaller than the degree of I_{Ks} potentiation under control conditions (97.1 ± 11.9% increase, $n=16$; $P<0.05$; Figure 4). A similar degree of I_{Ks} potentiation by phenylephrine (30 μM) was observed in atrial myocytes pretreated for 5–10 min with higher concentration (1 μM) of BIS-I (40.3 ± 6.1% increase, $n=5$; Figure 4). These results support an involvement of PKC activation in the potentiation of I_{Ks} via α_1-adrenoceptors in guinea-pig atrial myocytes. Bath application of BIS-I at concentrations of 100 nM and 1 μM alone reduced the amplitude of basal I_{Ks} by 10.1 ± 3.2 ($n=6$) and 11.1 ± 3.0% ($n=5$), respectively, which appears to be consistent with a recent report showing a modest (12%) reduction of I_{Ks} by exposure to BIS-I (1 μM) in guinea-pig ventricular myocytes (Missan *et al.*, 2006).

Immunoblotting study with the use of isoform-specific antibody has detected the expression of at least five different PKC isoforms, namely α, βII, γ, ε and ζ in guinea-pig heart (Takeishi *et al.*, 1999). To elucidate which isoform(s) of PKC is involved in the I_{Ks} response to phenylephrine, we used three isoform-selective pharmacological inhibitors of PKC, namely Gö-6976 (Martiny-Baron *et al.*, 1993), Gö-6983 (Gschwendt *et al.*, 1996) and rottlerin (Gschwendt *et al.*, 1994). Figure 3b illustrates a representative example of the I_{Ks} response to

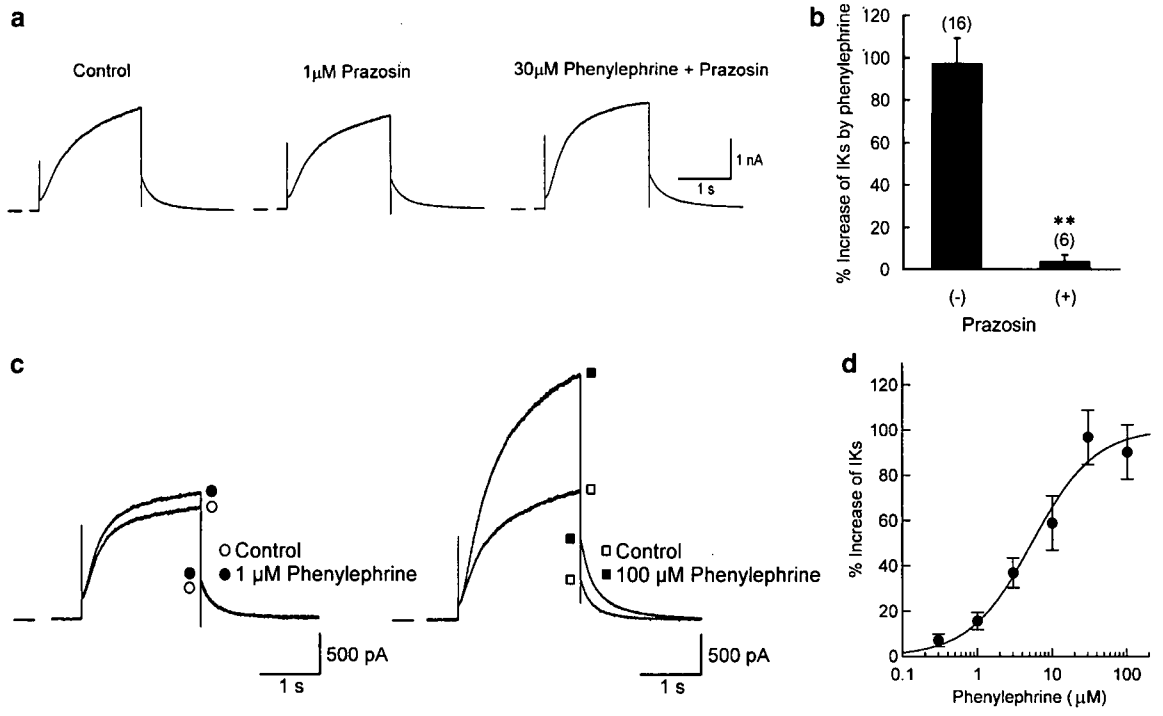

Figure 2 Potentiation of I_{Ks} by phenylephrine through α_1-adrenoceptor. (**a**) I_{Ks}, recorded in response to 2-s depolarization to +30 mV from a holding potential of −50 mV (the same voltage-clamp protocol as in Figure 1a), under control conditions (left panel), 5 min after exposure to 1 μM prazosin (middle) and 5 min after subsequent addition of 30 μM phenylephrine (right). (**b**) Percentage increase in I_{Ks} tail current, evoked by 30 μM phenylephrine in the absence and presence of 1 μM prazosin. $^{**}P<0.01$ compared with value in the absence of prazosin. (**c**) Superimposed current traces of I_{Ks} recorded using the same voltage-clamp protocol as in Figure 2a, before and ~5 min after exposure to phenylephrine at concentration of 1 (left panel) or 100 μM (right). These records were obtained from different myocytes. (**d**) Concentration–response relationship for the potentiation of I_{Ks} by phenylephrine. Percentage increase in I_{Ks} tail current was measured for each concentration (0.3–100 μM) of phenylephrine. Each data point represents mean values±s.e.m. of 3–6 myocytes and is fitted with a Hill equation, yielding EC_{50} of 5.4 μM and n_H of 1.03. Only one concentration of phenylephrine was examined in a given myocyte to exclude possible complications of desensitization.

phenylephrine in the presence of the indolocarbazole Gö-6976, which largely inhibits Ca^{2+}-dependent (α, β and γ) but not Ca^{2+}-independent (δ, ε and ζ) isoforms when used at a concentration of 100 nM (Martiny-Baron *et al.*, 1993). The potentiation of I_{Ks} was not significantly influenced by the addition of 100 nM Gö-6976 (78.4±9.0% increase, $n=6$; Figure 4) when compared with control, suggesting that conventional PKC isoforms (α, β and γ) were little, if at all, involved in the response. Similarly, the stimulatory action of phenylephrine was not significantly affected by the bisindolylmaleimide Gö-6983 at 100 nM (Figures 3c and 4; 79.8±11.6% increase, $n=6$), which at this concentration inhibits conventional (α, β and γ), novel (δ) and atypical (ζ) PKC isoforms (Gschwendt *et al.*, 1996). In addition, I_{Ks} response to phenylephrine was practically insensitive to 10 μM rottlerin (Figures 3d and 4; 84.9±8.2% increase, $n=6$), which potently inhibits PKCδ but not PKCε at the concentration tested (Gschwendt *et al.*, 1994). Based on these differences in the sensitivity of phenylephrine action to pharmacological inhibitors, PKCε isoform appears to be involved in mediating the stimulatory effect of phenylephrine on I_{Ks} in guinea-pig atrial myocytes.

We further tested the effects of the peptide translocation inhibitors of PKC isoforms βC2-4 (Ron *et al.*, 1995) and εV1-2 (Johnson *et al.*, 1996) on the stimulatory action of phenylephrine on I_{Ks}. It is generally accepted that upon activation, each PKC isoform translocates and binds to the specific anchoring proteins referred to as RACKs (receptors for activated C kinases) within a cell (Mochly-Rosen and Gordon, 1998). The interaction between conventional PKC isoforms and their RACKs is mediated in part by the C2 domain, whereas the binding of the C2-less novel PKC isoforms to their RACKs is via the V1 domain (Mochly-Rosen and Gordon, 1998). The peptide fragment βC2-4, which comprises nine amino acids (SLNPEWNET) derived from the C2 region of PKCβ(218–226), specifically inhibits the translocation of C2-containing conventional PKC isoforms (α, β and γ) but not that of C2-lacking novel PKC isoforms (δ and ε; Ron *et al.*, 1995). On the other hand, the peptide εV1-2 is composed of eight amino acids (EAVSLKPT) that are derived from the V1 region of PKCε and specifically prevents translocation of PKCε to its RACKs (Johnson *et al.*, 1996). Previous patch-clamp studies have demonstrated that intracellular application of these peptide inhibitors at a concentration of 100 nM is effective at significantly reducing the action of PKC isoform(s) on ion channels in mammalian cardiac myocytes (Zhang *et al.*, 1997; Hool, 2000; Xiao *et al.*, 2001). After allowing ~10 min for the pipette solution containing βC2-4 or εV1-2 to diffuse into the cell inside, the effect of phenylephrine on I_{Ks} was tested. As demonstrated in Figure 3e and f, the stimulatory action of phenylephrine was not appreciably influenced by 100 nM

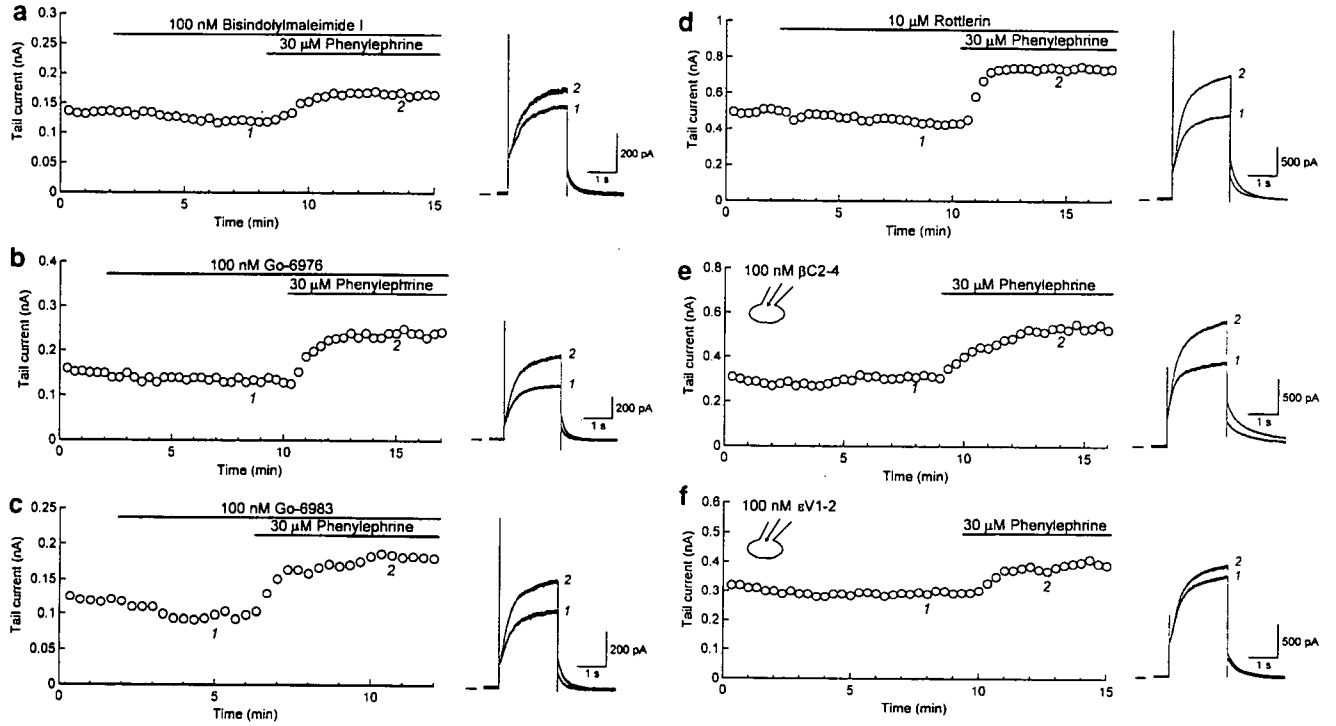

Figure 3 Effect of PKC isoform inhibition on the stimulatory action of phenylephrine on I_{Ks}. (**a**, **b**, **c** and **d**) Atrial myocytes were initially exposed to 100 nM BIS-I (**a**), 100 nM Gö-6976 (**b**), 100 nM Gö-6983 (**c**) or 10 μM rottlerin (**d**) for 5–10 min and then to 30 μM phenylephrine, as indicated by the horizontal bars. (**e** and **f**) Atrial myocytes were dialyzed with a pipette solution containing 100 nM βC2-4 (**e**) or 100 nM εV1-2 (**f**) for approximately 10 min before exposure to 30 μM phenylephrine. I_{Ks} was repetitively (every 20 s) activated by depolarizing steps to +30 mV from a holding potential of −50 mV, and amplitude of the tail current, measured upon return to the holding potential was plotted.

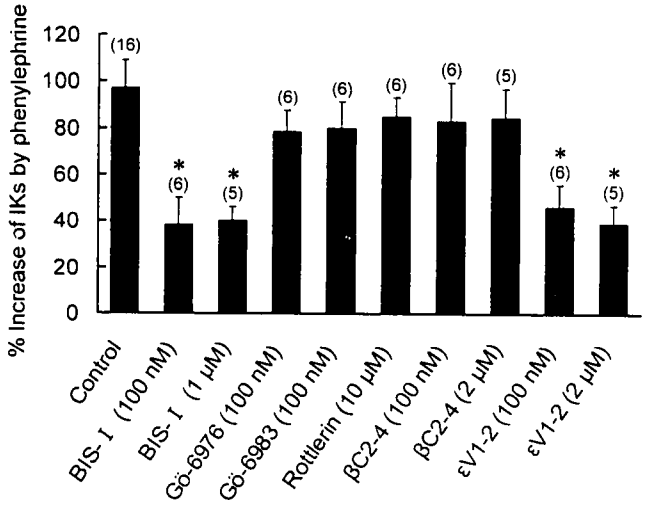

Figure 4 Summary bar graph showing the percentage increase in the amplitude of I_{Ks} tail current by phenylephrine in control and in the presence of pharmacological and peptide inhibitors of PKC isoforms. Effect of each inhibitor was compared with control (*$P<0.05$ vs control).

βC2-4 (83.0±16.6% increase, $n=6$; Figure 4), but was significantly reduced by 100 nM εV1-2 (46.4±9.2% increase, $n=6$; Figure 4). Similarly, I_{Ks} response to phenylephrine was significantly reduced by εV1-2 (39.2±7.7% increase, $n=5$) but not by βC2-4 (84.5±12.5% increase, $n=5$), when applied at higher concentration (2 μM, Figure 4). These experiments with PKC isoform-selective peptide inhibitors again support a significant role for PKCε in mediating the potentiation of I_{Ks} by phenylephrine.

PKCε also mediates the potentiation of I_{Ks} by phorbol ester

In the next series of experiments, we explored which isoform(s) of PKC was primarily involved in the I_{Ks} response to PMA, by examining the effects of βC2-4 and εV1-2 added to a pipette solution. Figure 5a illustrates a representative time course for the potentiation of I_{Ks} by bath application of PMA (100 nM) under control conditions. A peak response was typically attained ~5–10 min after starting the application of PMA and was sustained for at least 5 min even after washout of the compound. In a total of six myocytes, bath application of 100 nM PMA increased I_{Ks} by 64.2±1.3% (Figure 5g), when evaluated by the amplitude of tail current at a test potential of +30 mV. This stimulatory action of PMA (100 nM) was almost totally blocked by pretreatment with 100 nM BIS-I (2.7±1.3% increase, $n=6$; Figure 5b and g), supporting the view that activation of PKC mediates potentiation of I_{Ks} by PMA. Figure 5c demonstrates superimposed current traces of I_{Ks} recorded during 2-s depolarizing steps to potentials between −40 and +50 mV, before and after ~10 min exposure to 100 nM PMA. As illustrated in Figure 5d, PMA increased the amplitude of I_{Ks} tail currents at all potentials tested. The voltage dependence of I_{Ks} activation was little affected by exposure to PMA (control, $V_{1/2}=5.0\pm2.2$ mV, $k=11.9\pm1.4$ mV; PMA, $V_{1/2}=5.9\pm1.8$ mV, $k=12.5\pm1.5$ mV, $n=4$).

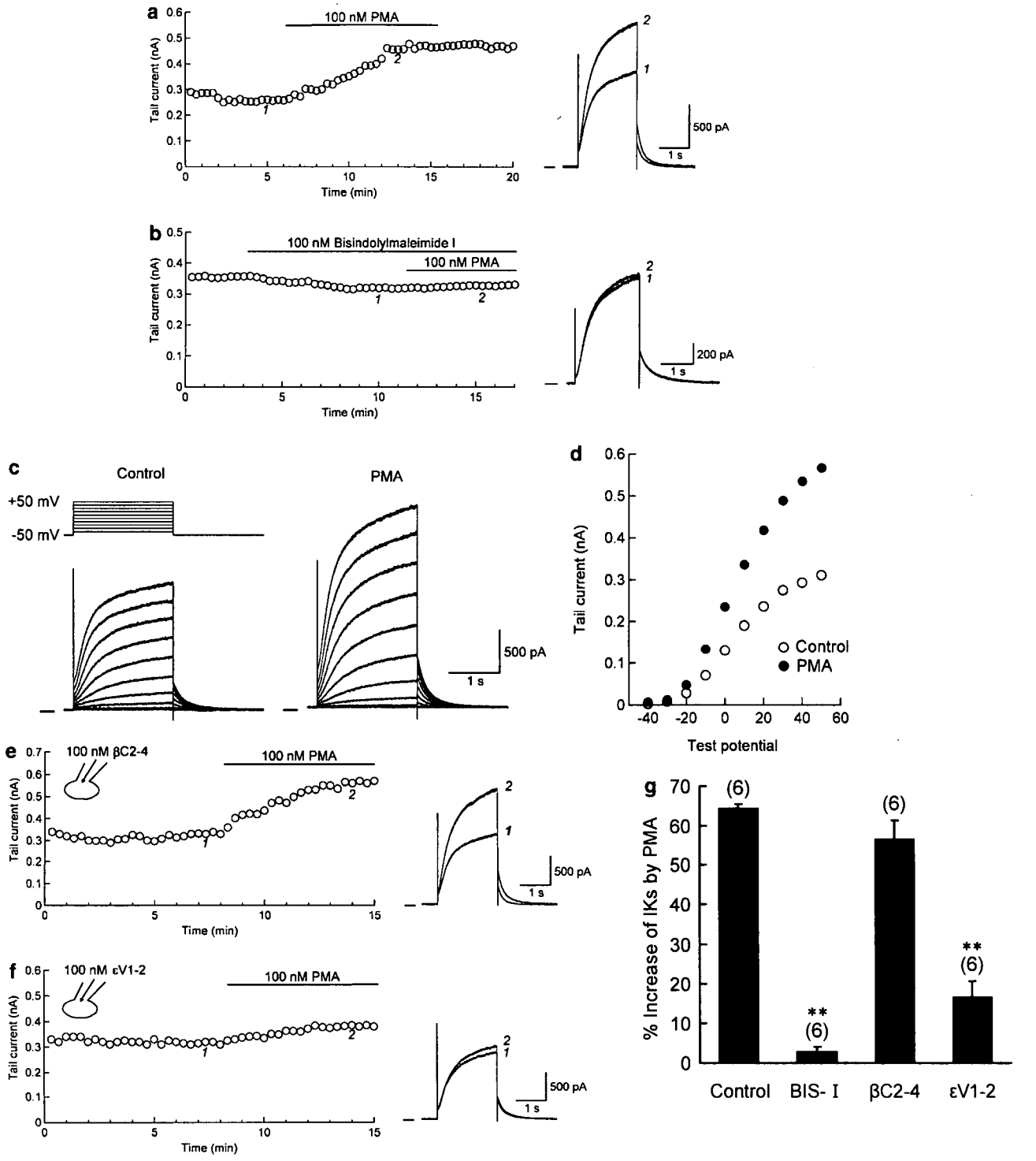

Figure 5 PKCε is primarily involved in the stimulatory action of PMA on I_{Ks}. (**a** and **b**) Time course of changes in the amplitude of I_{Ks} tail current during exposure to 100 nM PMA without (**a**) or with (**b**) pretreatment with 100 nM BIS-I. I_{Ks} was repetitively (every 20 s) activated by 2-s depolarizing steps to + 30 mV. (**c**) Superimposed current traces of I_{Ks} activated at test potentials of −40 to + 50 mV, before and ~10 min after exposure to 100 nM PMA. (**d**) *I–V* relationships for I_{Ks} tail currents, obtained from the experiments shown in (**c**). (**e** and **f**) Time courses in the changes in I_{Ks} tail currents recorded from an atrial myocyte dialyzed with a pipette solution containing 100 nM βC2-4 (**e**) or 100 nM εV1-2 (**f**). (**g**) Summary bar graph showing the percentage increase in the amplitude of I_{Ks} tail currents by PMA, in control and in the presence of BIS-I (100 nM, bath), βC2-4 (100 nM, pipette) or εV1-2 (100 nM, pipette). Effect of each inhibitor was compared with control (**$P<0.01$ vs control).

Figure 5e and f, respectively, shows a typical example of I_{Ks} response to 100 nM PMA in an atrial myocyte dialyzed with a pipette solution containing βC2-4 (100 nM) and εV1-2 (100 nM). The stimulatory effect of PMA was minimally affected by βC2-4 (56.7±4.7% increase, $n=6$) but was significantly attenuated by εV1-2 (16.5±4.0% increase, $n=6$), compared with the control value (64.2±1.3% increase, $n=6$; Figure 5g). These results indicate that PKCε is

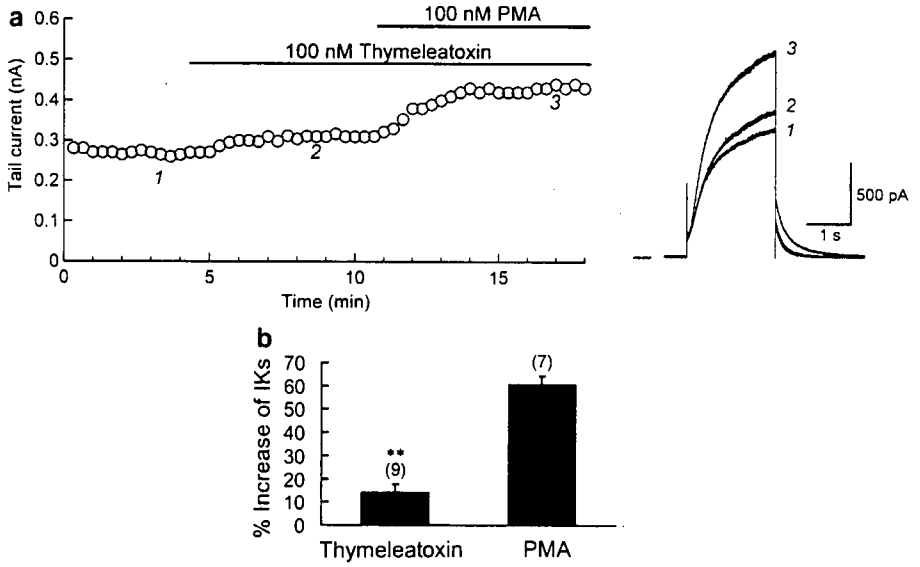

Figure 6 Effects of thymeleatoxin and PMA on I_{Ks}. (**a**) Time course of changes in the amplitude of I_{Ks} during exposure to PMA in the presence of thymeleatoxin. (**b**) Summary bar graph showing the percentage increase in the amplitude of I_{Ks} tail currents, evoked by thymeleatoxin (100 nM) alone, and PMA (100 nM) in the presence of thymeleatoxin. The values are calculated with reference to the baseline amplitude of I_{Ks} tail current. $^{**}P<0.01$ compared between these two groups.

also predominantly involved in the potentiation of I_{Ks} by PMA-induced PKC activation in guinea-pig atrial myocytes.

The experimental results obtained using pharmacological and peptide inhibitors for PKC isoforms indicate that activation of conventional PKCs (α, βI, βII and γ) is not primarily involved in the potentiation of I_{Ks} by the α_1-adrenergic agonist phenylephrine and the phorbol ester PMA in guinea-pig atrial myocytes. To substantiate this view, we examined the response of I_{Ks} to thymeleatoxin, a phorbol derivative which predominantly activates conventional PKC isoforms (Ryves *et al.*, 1991). Bath application of 100 nM thymeleatoxin only slightly increased the amplitude of I_{Ks} by 14.1±3.4% ($n=9$; Figure 6a and b), which was usually attained within 5–10 min after starting the application. However, subsequent addition of 100 nM PMA in the continued presence of 100 nM thymeleatoxin caused an additional significant increase in I_{Ks} by 60.8±3.6% ($n=7$) of the baseline amplitude (Figure 6b). This finding again supports a predominant role of novel PKC (PKCε) over conventional PKCs in the potentiation of I_{Ks} in guinea-pig atrial myocytes.

Discussion

The present study demonstrates that I_{Ks} is markedly (approximately twofold) potentiated by phenylephrine (30 μM) through α_1-adrenoceptors in guinea-pig atrial myocytes (Figure 2). The stimulatory action of phenylephrine was significantly, if not completely, reduced by the general PKC inhibitor BIS-I (Figures 3a and 4), which strongly suggests that PKC activation plays an important role in mediating the α_1-adrenoceptor-induced I_{Ks} potentiation. Western-blot analysis using an antibody specific to PKC isoform has suggested that α_1-adrenoceptor stimulation with phenylephrine causes translocation and thereby activation of both conventional and novel isoforms of PKC in native cardiac myocytes (Ruf *et al.*, 2002). On the other hand, in the present study we found that the stimulatory action of phenylephrine on I_{Ks} was significantly reduced by the PKCε-selective inhibitory peptide (εV1-2) but was little affected by the peptide inhibitor (βC2-4) for all conventional PKC isoforms (α, β and γ), which favours a preferential role for the novel isoform PKCε (Figures 3e, f and 4). This view is also supported by the experiments showing that the stimulatory action of phenylephrine was minimally affected by the indolocarbazole Gö-6976 (Figures 3b and 4), which is believed to have the highest selectivity for conventional PKC isoforms among the pharmacological inhibitors currently available (Martiny-Baron *et al.*, 1993). The present investigation also confirms a substantial enhancement of I_{Ks} by phorbol ester PMA (Figures 5 and 6), which directly activates both conventional and novel isoforms of PKC, independent of receptor stimulation. This PMA action on I_{Ks} was also significantly reduced by εV1-2 but not by βC2-4 (Figure 5), again supporting a functional role of PKCε in the regulation of cardiac I_{Ks}.

Voltage-clamp study using the *Xenopus* oocyte expression system has clearly demonstrated that both PKCβII and PKCε, but not PKCα, PKCβI, PKCδ and PKCη, are involved in the PMA-induced potentiation of heteromeric KCNQ1/KCNE1 channels (Xiao *et al.*, 2003), molecular constituents of human I_{Ks} (Barhanin *et al.*, 1996; Sanguinetti *et al.*, 1996). On the other hand, it was observed in guinea-pig ventricular myocytes that the delayed rectifier K^+ current, I_K (which seems to largely comprise I_{Ks}), is increased by exogenous application of the type III (α) PKC purified from bovine whole brain (Tohse *et al.*, 1990), which resembles the structure of PKCα (Kikkawa *et al.*, 1987). These observations appear to be apparently distinct from the present results, concerning the functional role of PKCα or PKCβII in the regulation of I_{Ks}. Individual PKC isoforms (α, βI, βII, δ,

ε and ζ) in native cardiac myocytes have a differential localization before and after stimulation by norepinephrine or PMA (Disatnik *et al.*, 1994). Whereas PKCα and PKCβII translocate from the cytosolic region to the perinuclear region and/or cell periphery, PKCε, upon stimulation, typically translocates to cross-striated regions in ventricular myocytes, which places it near the transverse tubules (t-tubules). Evidence has been presented to indicate that minK (KCNE1) proteins, important function-modifying ancillary β-subunit of the I_{Ks} channel, are preferentially localized in the t-tubules in native ventricular myocytes (Furukawa *et al.*, 2001). It is probable that the colocalization of activated PKCε with I_{Ks} channel proteins underlies the selective potentiation of I_{Ks} by PKCε in native cardiac myocytes. Further work is required to examine the localization of PKCε and I_{Ks} channel subunits in atrial myocytes, which lack an extensive t-tubule network.

In the present study, BIS-I at 100 nM almost totally abolishes the potentiation of I_{Ks} by PMA (Figure 5b and g) but partially reduces the stimulatory action of phenylephrine on I_{Ks} even when applied at 1 μM (Figure 4). We have previously demonstrated that I_{Ks} in guinea-pig atrial myocytes is increased by intracellular application of anti-phosphatidylinositol 4,5-bisphosphate (PtdIns(4,5)P_2) antibody but is decreased by intracellular addition of exogenous PtdIns(4,5)P_2 (Ding *et al.*, 2004). These observations suggest that endogenous membrane PtdIns(4,5)P_2 exerts an inhibitory action on I_{Ks}. We further showed that stimulatory action of extracellular ATP on I_{Ks} is due, at least partly, to the reduction of membrane PtdIns(4,5)P_2 which is likely to occur following the stimulation of P2Y receptors coupled to a Gq-phospholipase C (PLC) signaling pathway (Ding *et al.*, 2004). It is therefore possible that, in addition to PKC activation, the stimulation of Gq-PLC-coupled α_1-adrenoceptors causes other signaling events such as depletion of membrane PtdIns(4,5)P_2, to potentiate I_{Ks} in atrial myocytes. It is of interest to evaluate the relative contribution of PKC activation and membrane PtdIns(4,5)P_2 depletion to the potentiation of I_{Ks} observed during the stimulation of various kinds of Gq-PLC-coupled receptors expressed in the heart.

The maximal response of I_{Ks} to phenylephrine in atrial myocytes (97.1±11.9% increase) appears to be considerably larger than that in ventricular myocytes of same species (29.9±9.1% increase; Tohse *et al.*, 1992). On the other hand, it has been demonstrated in guinea-pig ventricular myocytes that the amplitude of I_{Ks} is potentiated by ~45–60% by bath application of phorbol esters PMA (also referred to as 12-*O*-tetradecanoylphorbol 13-acetate, TPA) and phorbol 12,13-dibutyrate (PDBu) (Walsh and Kass, 1988; Tohse *et al.*, 1990; Yazawa and Kameyama, 1990). It is thus likely that I_{Ks} can be enhanced by an almost similar degree in atrial and ventricular myocytes of guinea-pigs when PKC is directly activated by phorbol esters. As judged from these observations, it is likely that, following the stimulation of α_1-adrenoceptors, PKC may be more effectively activated to potentiate I_{Ks} in atrial myocytes. Further studies should be conducted to determine the relative efficiency of α_1-adrenoceptor stimulation in potentiating I_{Ks} in atrial and ventricular myocytes under the same experimental conditions, including methods to isolate I_{Ks} from total I_K.

Previous investigators have reported that PKC activation causes a species-specific effect on cardiac I_{Ks}; PKC stimulation increases I_{Ks} in guinea-pigs but decreases the current amplitude in most of the other mammalian species (Varnum *et al.*, 1993; Robinson *et al.*, 2000). This difference has been accounted for, at least partly, by the sequence variation of minK (KCNE1) protein (Varnum *et al.*, 1993); a PKC phosphorylation site (Ser-102), which is responsible for current reduction, is absent in guinea-pigs but is present in other mammalian species including humans. In recent years, however, Kathöfer *et al.* (2003) have demonstrated that PKC activation increases membrane current through the human KCNQ1/KCNE1 channel. Furthermore, these authors detected, using site-directed mutagenesis experiments, the PKC phosphorylation sites (Ser-409, Ser-464, Thr-513 and Ser-577) in a pore-forming α-subunit, KCNQ1 protein, which contributes to PKC-dependent increase in KCNQ1/KCNE1 current. Future studies are required to examine whether the PKCε-mediated I_{Ks} potentiation is present and functions in native cardiac myocytes of various mammalian species including humans.

A number of experimental and/or clinical studies have strongly suggested that, whereas increased expression of PKCβI and/or PKCβII is implicated in the development of cardiomyopathy (Wakasaki *et al.*, 1997) and heart failure (Bowling *et al.*, 1999), the activation and translocation of PKCε confers cardioprotection that is associated with ischemic preconditioning (Gray *et al.*, 1997; Qiu *et al.*, 1998; Liu *et al.*, 1999). Furthermore, a recent study has found that intracoronary injection of a selective PKCε-activating peptide, ψεRACK, not only reduces infarct size but also suppresses the occurrence of ventricular tachyarrhythmias caused by ischemia–reperfusion in porcine hearts (Inagaki *et al.*, 2005). In atrial and ventricular myocardium, I_{Ks} activation plays a major role in determining the action potential duration that controls the amount of Ca^{2+} influx through simultaneously activated $I_{Ca,L}$ (Pennefather and Cohen, 1990). It seems, therefore reasonable to speculate that activation of PKCε and resultant stimulation of I_{Ks} can reduce the amount of Ca^{2+} influx during action potentials and thereby spare energy required for intracellular Ca^{2+} handling, which can be beneficial to the cardiomyocytes, especially in condition where the oxygen supply to cardiac muscle becomes inadequate (hypoxia or ischemia). It will be interesting to elucidate whether PKCε-mediated potentiation of I_{Ks} described here in atrial myocytes can be applicable to the I_{Ks} regulation in cardiac ventricular myocytes of mammalian species including humans and constitutes, at least in part, the cardioprotective action of PKCε during ischemic preconditioning and/or ischemia–reperfusion.

In conclusion, our data indicate that the ε isoform of PKC (PKCε) is predominantly involved in the stimulatory action of PKC on I_{Ks} and contributes to α_1-adrenergic potentiation of I_{Ks} in native guinea-pig atrial myocytes.

Acknowledgements

This study was supported by Grant-in-Aid for Scientific Research from Japan Society for the Promotion of Science.

Conflict of interest

The authors state no conflict of interest.

References

Barhanin J, Lesage F, Guillemare E, Fink M, Lazdunski M, Romey G (1996). K_VLQT1 and IsK (minK) proteins associate to form the I_{Ks} cardiac potassium current. *Nature* **384**: 78–80.

Bosch RF, Gaspo R, Busch AE, Lang HJ, Li GR, Nattel S (1998). Effects of the chromanol 293B, a selective blocker of the slow, component of the delayed rectifier K^+ current, on repolarization in human and guinea pig ventricular myocytes. *Cardiovasc Res* **38**: 441–450.

Bosch RF, Schneck AC, Csillag S, Eigenberger B, Gerlach U, Brendel J *et al.* (2003). Effects of the chromanol HMR 1556 on potassium currents in atrial myocytes. *Naunyn-Schmiedebergs Arch Pharmacol* **367**: 281–288.

Bowling N, Walsh RA, Song G, Estridge T, Sandusky GE, Fouts RL *et al.* (1999). Increased protein kinase C activity and expression of Ca^{2+}-sensitive isoforms in the failing human heart. *Circulation* **99**: 384–391.

Ding WG, Toyoda F, Matsuura H (2004). Regulation of cardiac I_{Ks} potassium current by membrane phosphatidylinositol 4,5-bisphosphate. *J Biol Chem* **279**: 50726–50734.

Disatnik M-H, Buraggi G, Mochly-Rosen D (1994). Localization of protein kinase C isozymes in cardiac myocytes. *Exp Cell Res* **210**: 287–297.

Fabiato A, Fabiato F (1979). Calculator programs for computing the composition of the solutions containing multiple metals and ligands used for experiments in skinned muscle cells. *J Physiol (Paris)* **75**: 463–505.

Furukawa T, Ono Y, Tsuchiya H, Katayama Y, Bang ML, Labeit D *et al.* (2001). Specific interaction of the potassium channel β-subunit minK with the sarcomeric protein T-cap suggests a T-tubule-myofibril linking system. *J Mol Biol* **313**: 775–784.

Gintant GA (1996). Two components of delayed rectifier current in canine atrium and ventricle. Does IKs play a role in the reverse rate dependence of class III agents? *Circ Res* **78**: 26–37.

Gray MO, Karliner JS, Mochly-Rosen D (1997). A selective ε-protein kinase C antagonist inhibits protection of cardiac myocytes from hypoxia-induced cell death. *J Biol Chem* **272**: 30945–30951.

Gschwendt M, Dieterich S, Rennecke J, Kittstein W, Mueller HJ, Johannes FJ (1996). Inhibition of protein kinase C μ by various inhibitors. Differentiation from protein kinase c isoenzymes. *FEBS Lett* **392**: 77–80.

Gschwendt M, Müller HJ, Kielbassa K, Zang R, Kittstein W, Rincke G *et al.* (1994). Rottlerin, a novel protein kinase inhibitor. *Biochem Biophys Res Commun* **199**: 93–98.

Hamill OP, Marty A, Neher E, Sakmann B, Sigworth FJ (1981). Improved patch-clamp techniques for high-resolution current recording from cells and cell-free membrane patches. *Pflügers Arch* **391**: 85–100.

Han W, Wang Z, Nattel S (2001). Slow delayed rectifier current and repolarization in canine cardiac Purkinje cells. *Am J Physiol* **280**: H1075–H1080.

Hool LC (2000). Hypoxia increases the sensitivity of the L-type Ca^{2+} current to β-adrenergic receptor stimulation via a C2 region-containing protein kinase C isoform. *Circ Res* **87**: 1164–1171.

Inagaki K, Begley R, Ikeno F, Mochly-Rosen D (2005). Cardioprotection by ε-protein kinase C activation from ischemia: continuous delivery and antiarrhythmic effect of an ε-protein kinase C-activating peptide. *Circulation* **111**: 44–50.

Johnson JA, Gray MO, Chen CH, Mochly-Rosen D (1996). A protein kinase C translocation inhibitor as an isozyme-selective antagonist of cardiac function. *J Biol Chem* **271**: 24962–24966.

Johnson JA, Mochly-Rosen D (1995). Inhibition of the spontaneous rate of contraction of neonatal cardiac myocytes by protein kinase C isozymes. A putative role for the ε isozyme. *Circ Res* **76**: 654–663.

Kathöfer S, Röckl K, Zhang W, Thomas D, Katus H, Kiehn J *et al.* (2003). Human β_3-adrenoreceptors couple to KvLQT1/MinK potassium channels in *Xenopus* oocytes via protein kinase C phosphorylation of the KvLQT1 protein. *Naunyn-Schmiedeberg's Arch Pharmacol* **368**: 119–126.

Kikkawa U, Ono Y, Ogita K, Fujii T, Asaoka Y, Sekiguchi K *et al.* (1987). Identification of the structures of multiple subspecies of protein kinase C expressed in rat brain. *FEBS Lett* **217**: 227–231.

Li G-R, Feng J, Yue L, Carrier M, Nattel S (1996). Evidence for two components of delayed rectifier K^+ current in human ventricular myocytes. *Circ Res* **78**: 689–696.

Liu GS, Cohen MV, Mochly-Rosen D, Downey JM (1999). Protein kinase C-ε is responsible for the protection of preconditioning in rabbit cardiomyocytes. *J Mol Cell Cardiol* **31**: 1937–1948.

Martiny-Baron G, Kazanietz MG, Mischak H, Blumberg PM, Kochs G, Hug H *et al.* (1993). Selective inhibition of protein kinase C isozymes by the indolocarbazole Gö 6976. *J Biol Chem* **268**: 9194–9197.

Matsuura H, Tsuruhara Y, Sakaguchi M, Ehara T (1996). Enhancement of delayed rectifier K^+ current by P_2-purinoceptor stimulation in guinea-pig atrial cells. *J Physiol (London)* **490**: 647–658.

Mellor H, Parker PJ (1998). The extended protein kinase C superfamily. *Biochem J* **332**: 281–292.

Missan S, Linsdell P, McDonald TF (2006). Tyrosine kinase and phosphatase regulation of slow delayed-rectifier K^+ current in guinea-pig ventricular myocytes. *J Physiol (London)* **573**: 469–482.

Mochly-Rosen D, Gordon AS (1998). Anchoring proteins for protein kinase C: a means for isozyme selectivity. *FASEB J* **12**: 35–42.

Pennefather P, Cohen IS (1990). Molecular mechanisms of cardiac K^+-channel regulation. In: Zipes DP, Jalife J (eds). *Cardiac Electrophysiology from Cell to Bedside*. WB Saunders: Philadelphia, pp 17–28.

Powell T, Terrar DA, Twist VW (1980). Electrical properties of individual cells isolated from adult rat ventricular myocardium. *J Physiol (London)* **302**: 131–153.

Pucéat M, Hilal-Dandan R, Strulovici B, Brunton LL, Brown JH (1994). Differential regulation of protein kinase C isoforms in isolated neonatal and adult rat cardiomyocytes. *J Biol Chem* **269**: 16938–16944.

Qiu Y, Ping P, Tang X-L, Manchikalapudi S, Rizvi A, Zhang J *et al.* (1998). Direct evidence that protein kinase C plays an essential role in the development of late preconditioning against myocardial stunning in conscious rabbits and that epsilon is the isoform involved. *J Clin Invest* **101**: 2182–2198.

Robinson RB, Liu QY, Rosen MR (2000). Ionic basis for action potential prolongation by phenylephrine in canine epicardial myocytes. *J Cardiovasc Electrophysiol* **11**: 70–76.

Ron D, Luo J, Mochly-Rosen D (1995). C2 region-derived peptides inhibit translocation and function of β protein kinase C *in vivo*. *J Biol Chem* **270**: 24180–24187.

Ruf S, Piper M, Schluter KD (2002). Specific role for the extracellular signal-regulated kinase pathway in angiotensin II- but not phenylephrine-induced cardiac hypertrophy *in vitro*. *Pflügers Arch* **443**: 483–490.

Rybin VO, Steinberg SF (1994). Protein kinase C isoform expression and regulation in the developing rat heart. *Circ Res* **74**: 299–309.

Ryves WJ, Evans AT, Olivier AR, Parker PJ, Evans FJ (1991). Activation of the PKC-isotypes α, β_1, γ, δ and ε by phorbol esters of different biological activities. *FEBS Lett* **288**: 5–9.

Sanguinetti MC, Curran ME, Zou A, Shen J, Spector PS, Atkinson DL *et al.* (1996). Coassembly of K_VLQT1 and minK (IsK) proteins to form cardiac I_{Ks} potassium channel. *Nature* **384**: 80–83.

Sanguinetti MC, Jurkiewicz NK (1990). Two components of cardiac delayed rectifier K^+ current. Differential sensitivity to block by class III antiarrhythmic agents. *J Gen Physiol* **96**: 195–215.

Sanguinetti MC, Jurkiewicz NK (1991). Delayed rectifier outward K^+ current is composed of two currents in guinea pig atrial cells. *Am J Physiol* **260**: H393–H399.

Sanguinetti MC, Jurkiewicz NK, Scott A, Siegl PKS (1991). Isoproterenol antagonizes prolongation of refractory period by the class III antiarrhythmic agent E-4031 in guinea pig myocytes. Mechanism of action. *Circ Res* **68**: 77–84.

Stengl M, Volders PGA, Thomsen MB, Spätjens RLHMG, Sipido KR, Vos MA (2003). Accumulation of slowly activating delayed rectifier potassium current (I_{Ks}) in canine ventricular myocytes. *J Physiol (London)* **551**: 777–786.

Takeishi Y, Jalili T, Ball NA, Walsh RA (1999). Responses of cardiac protein kinase C isoforms to distinct pathological stimuli are differentially regulated. *Circ Res* **85**: 264–271.

Takeishi Y, Ping P, Bolli R, Kirkpatrick DL, Hoit BD, Walsh RA (2000). Transgenic overexpression of constitutively active protein kinase C ε causes concentric cardiac hypertrophy. *Circ Res* **86**: 1218–1223.

Terrenoire C, Clancy CE, Cormier JW, Sampson KJ, Kass RS (2005). Autonomic control of cardiac action potentials: role of potassium channel kinetics in response to sympathetic stimulation. *Circ Res* **96**: e25–e34.

Tohse N, Kameyama M, Sekiguchi K, Shearman MS, Kanno M (1990). Protein kinase C activation enhances the delayed rectifier potassium current in guinea-pig heart cells. *J Mol Cell Cardiol* **22**: 725–734.

Tohse N, Nakaya H, Kanno M (1992). α_1-Adrenoceptor stimulation enhances the delayed rectifier K^+ current of guinea pig ventricular cells through the activation of protein kinase C. *Circ Res* **71**: 1441–1446.

Toullec D, Pianetti P, Coste H, Bellevergue P, Grand-Perret T, Ajakane M *et al.* (1991). The bisindolylmaleimide GF 109203X is a potent and selective inhibitor of protein kinase C. *J Biol Chem* **266**: 15771–15781.

Tsien RY, Rink TJ (1980). Neutral carrier ion-selective microelectrodes for measurement of intracellular free calcium. *Biochim Biophys Acta* **599**: 623–638.

Varnum MD, Busch AE, Bond CT, Maylie J, Adelman JP (1993). The min K channel underlies the cardiac potassium current I_{Ks} and mediates species–specific responses to protein kinase C. *Proc Natl Acad Sci USA* **90**: 11528–11532.

Volders PGA, Stengl M, van Opstal JM, Gerlach U, Spätjens RLHMG, Beekman JDM *et al.* (2003). Probing the contribution of I_{Ks} to canine ventricular repolarization: key role for β-adrenergic receptor stimulation. *Circulation* **107**: 2753–2760.

Wakasaki H, Koya D, Schoen FJ, Jirousek MR, Ways DK, Hoit BD *et al.* (1997). Targeted overexpression of protein kinase C β2 isoform in myocardium causes cardiomyopathy. *Proc Natl Acad Sci USA* **94**: 9320–9325.

Walsh KB, Kass RS (1988). Regulation of a heart potassium channel by protein kinase A and C. *Science* **242**: 67–69.

Wang Z, Fermini B, Nattel S (1993). Delayed rectifier outward current and repolarization in human atrial myocytes. *Circ Res* **73**: 276–285.

Xiao G-Q, Mochly-Rosen D, Boutjdir M (2003). PKC isozyme selective regulation of cloned human cardiac delayed slow rectifier K current. *Biochem Biophys Res Commun* **306**: 1019–1025.

Xiao G-Q, Qu Y, Sun Z-Q, Mochly-Rosen D, Boutjdir M (2001). Evidence for functional role of εPKC isozyme in the regulation of cardiac Na^+ channels. *Am J Physiol* **281**: C1477–C1486.

Yazawa K, Kameyama M (1990). Mechanism of receptor-mediated modulation of the delayed outward potassium current in guinea-pig ventricular myocytes. *J Physiol (London)* **421**: 135–150.

Zhang Z-H, Johnson JA, Chen L, El-Sherif N, Mochly-Rosen D, Boutjdir M (1997). C2 region-derived peptides of β-protein kinase C regulate cardiac Ca^{2+} channels. *Circ Res* **80**: 720–729.

ELSEVIER

International Journal of Cardiology 121 (2007) 239–248

International Journal of Cardiology

www.elsevier.com/locate/ijcard

A paradoxical effect of lidocaine for the N406S mutation of *SCN5A* associated with Brugada syndrome☆

Hideki Itoh[a,b], Keiko Tsuji[b], Tomoko Sakaguchi[b], Iori Nagaoka[b], Yuko Oka[b], Yuko Nakazawa[b], Takenori Yao[b], Hikari Jo[b], Takashi Ashihara[b], Makoto Ito[b], Minoru Horie[b], Keiji Imoto[a,*]

[a] *Department of Information Physiology, National Institute for Physiological Sciences, Myodaiji, Okazaki 444-8787, Japan*
[b] *Heart Rhythm Center, Department of Cardiovascular and Respiratory Medicine, Shiga University of Medical Science, Seta Tsukinowa-cho, Otsu 520-2192, Japan*

Received 1 July 2006; received in revised form 8 January 2007; accepted 16 February 2007
Available online 18 April 2007

Abstract

Background: Accelerated intermediate inactivation, which is caused by mutations in the cardiac voltage-gated sodium channel α-subunit gene (*SCN5A*), is one of the molecular mechanisms underlying Brugada syndrome. The N406S mutation associated with Brugada syndrome results in the accelerated intermediate inactivation, in addition to unique pharmacological characteristics.
Methods: Functional sodium channels were expressed transiently in HEK293 cells by transfecting equally the α- and β-subunit plasmids (1 μg/ml) and the sodium current were measured in whole-cell mode of patch-clamp recording.
Results: Since the N406S mutant channel has a greatly reduced use-dependent block of lidocaine, we took the advantage of the mutant channel to examine the effect of lidocaine on intermediate inactivation using wild-type (WT) and N406S mutant channels recombinantly expressed in HEK293 cells. Lidocaine (100 μM) slowed the recovery from the fast inactivation similarly for WT and N406S. On the other hand, whereas lidocaine slowed the recovery from the intermediate inactivation for WT, lidocaine accelerated the recovery for N406S. Activity-dependent loss of channel availability by repetitive 500-ms pulses was more strongly enhanced and accelerated by lidocaine for WT, but lidocaine exerted little effect on the N406S channel.
Conclusion: We demonstrate that lidocaine may suppress Brugada syndrome associated with the N406S mutation by preventing the sodium channel from accumulating in the intermediate inactivation state.

Keywords: Brugada syndrome; Sodium channel; *SCN5A*; Lidocaine; Inactivation

Brugada syndrome is characterized by the ST-segment elevation in the V1 to V3 leads and nocturnal ventricular fibrillation [1]. Although only implantable cardioverter defibrillator (ICD) can prevent patients with Brugada syndrome from sudden cardiac death [2], ICD cannot prevent the occurrence of ventricular fibrillation. Therefore ICD is unable to decrease distress for symptomatic patients with Brugada syndrome. Belhassen et al. [3] reported that quinidine can prevent ventricular fibrillation induction in patients with Brugada syndrome. However, this therapy is not realistic because patients have to take a high dose for quinidine (1500 mg/day) and it is possible that side effects of quinidine appear easily.

The genetic basis of Brugada syndrome has been shown to be partly molecular defects in the gene *SCN5A* encoding the α subunit of the cardiac voltage-gated sodium channel ($Na_V1.5$) [4]. Several dozen of *SCN5A* mutations have been linked to the syndrome and shown to reduce the contribution of the sodium current (I_{Na}) during the early phases of the

☆ Presented in part at the 78th Scientific Sessions of AHA, Dallas, Texas, November 13, 2005, and published as an abstract (*Circulation*. 2005; 112: II-330).

* Corresponding author. Tel.: +81 564 59 5886; fax: +81 564 59 5891.
E-mail address: keijii@nips.ac.jp (K. Imoto).

0167-5273/$ - see front matter © 2007 Elsevier Ireland Ltd. All rights reserved.
doi:10.1016/j.ijcard.2007.02.007

action potential. Common underlying mechanisms are (1) failure to express, (2) reduced current due to a shift of voltage dependence, and (3) accelerated intermediate inactivation [5]. Antiarrhythmic drugs, especially class Ia or Ic drugs, are unfavorable for the patients with Brugada syndrome [6], because these drugs, by reducing I_{Na} furthermore, increase ST-segment elevation and induce ventricular tachycardia [7,8]. On the other hand, effects of class Ib antiarrhythmic drugs on sodium channels with Brugada mutations have not been well documented [6].

We previously reported a unique *SCN5A* mutation N406S, which is associated with multiple gating defects and with bidirectional effects on the blocking action of antiarrhythmic drugs [9]. Here we report the pharmacological effects of lidocaine on the N406S sodium channel expressed in a mammalian cell line. The mutation confers an unexpected interesting sensitivity to lidocaine on the sodium channel with the N406S mutation, and lidocaine prevents the N406S channel from accumulating in the state of intermediate inactivation.

1. Methods

1.1. Expression plasmids

The expression plasmids, pRc/CMV-hH1 (WT/hH1) and pGFP-IRES-hβ1 (β1) were kindly provided by Dr. A. L. George Jr. (Vanderbilt University, Nashville, TN). The mutations N406S were introduced using the QuickChange site-directed mutagenesis kit (Stratagene, La Jolla, CA) as previously demonstrated [9].

1.2. Cell transfection

Functional sodium channels were expressed transiently in HEK293 cells by transfecting equally the α- and β-subunit plasmids (1 μg/ml) unless otherwise stated. Cells were trysipnized, diluted with Dulbecco's modified Eagle's medium containing 10% fetal bovine serum, 30 units/ml penicillin and 30 μg/ml streptomycin. Cells were subjected to measurements 24–48 h after transfection. Cells expressing the sodium channels were selected through detection of GFP.

1.3. Electrophysiology

I_{Na} were measured in whole-cell mode of patch-clamp recording with an EPC-9 amplifier (HEKA, Lambrecht, Germany). Pipette resistance ranged from 1 to 2 MΩ when filled with the internal solution described below. The series resistance was electronically compensated at 70–85%. Both the leakage and the remaining capacitance were subtracted by the P/6 method, excluding the protocols for use-dependent block and 500-ms deporalization pulses to induce intermediate inactivation. The external solution contained (mM): 140 NaCl, 4 KCl, 2 $CaCl_2$, 1 $MgCl_2$, 10 HEPES, and 5 glucose (pH 7.4 with NaOH). The internal solution contained (mM): 100 CsF, 20 $CsCl_2$, 20 NaCl, 10 Hepes, and 5 EGTA (pH 7.4 with CsOH). Currents were

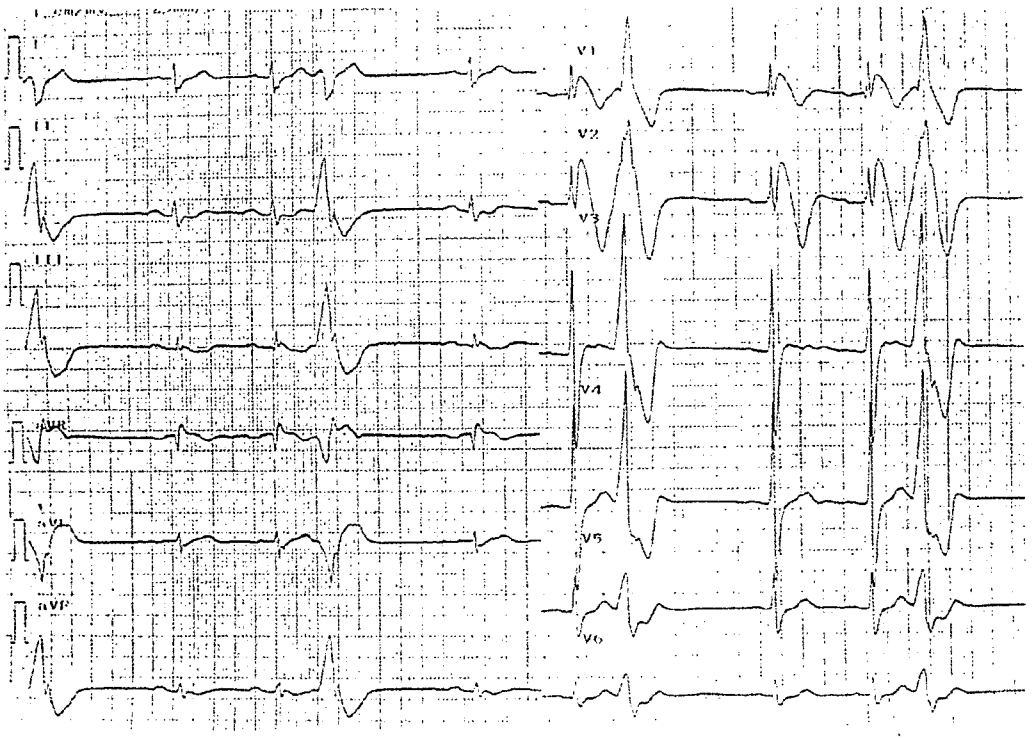

Fig. 1. Electrocardiogram after mexiletine was discontinued. ST-segment elevation was remarkable and premature ventricular contraction appeared.

digitized at 100 kHz after low-pass filtering at 10 kHz (−3 dB). Data were collected and analyzed using the Pulse software (HEKA) and Igor Pro (WaveMetrics, Lake Oswego, OR). The holding potential was maintained at −120 mV, unless otherwise described. Interval of pulse protocols were 1 to 5 s. All experiments were performed at room temperature.

The parameters for voltage dependence of activation were estimated from the current–voltage relation based on the equation: $I=G_{max}\times(V-V_{rev})/(1+\exp(-(V-V_{1/2})/k)$, where I is the peak current amplitude, G_{max} the maximum conductance, V test potential, V_{rev} the reversal potential, $V_{1/2}$ the midpoint of activation, and k the slope factor. Steady-state availability was fit with the Boltzmann equation, $I/I_{max}=1/(1+\exp((V-V_{1/2})/k))$ to determine the membrane potential for half-maximal inactivation $V_{1/2}$ and the slope factor k. Recovery from inactivation was analyzed by fitting data to a double exponential function: $I(t)/I_{max}=A_f\times(1-\exp(-t/\tau_f))+A_s\times(1-\exp(-t/\tau_s))$, where A_f and A_s the are the fractions of fast and slow inactivating components, respectively, and τ_f and τ_s are their time constants. All data were fit using a nonlinear least-squares minimization method.

1.4. Computer simulation

To understand the electrophysiological and pharmacological consequences of the N406S mutation, we constructed Markov models of the WT and N406S mutant sodium channels based on the experiment data of voltage-clamp recordings of sodium channels heterologously expressed in HEK 293 cells [9]. We tried the changes of parameters as small as possible. The models were then integrated into the Luo–Rudy theoretical model of the cardiac ventricular action potential. The simulations were encoded in C++ and implemented on a Pentium-4 computer running Windows XP or an HP Alpha system running Tru64 UNIX [10].

As a prototype channel model, we used the previously published Markov model of the cardiac sodium channel [11]. Because the mutant N406S showed no evidence of persistent opening, the lower states of the model were omitted. The Markov models for the WT and N406S sodium channels are shown in Fig. 8.

1.5. Statistical analysis

Results are presented as means±SE, and the statistical comparisons were made using the unpaired Student's t test. Statistical significance was assumed for $p<0.05$.

2. Results

2.1. Clinical characteristics

The N406S mutation was detected in a Brugada syndrome patient with unique pharmacological findings. The clinical profile of the patient was published previously [9]. He had taken mexiletine (300 mg/day) for 4 years because of frequent premature ventricular contractions. He did not have any ventricular tachycardias while he was on mexiletine. When mexiletine was discontinued, ST-segment elevation in leads V1 and V2 (type 1, coved type [12]) became remarkable (Fig. 1). The electrocardiogram did not show ST-segment elevation in the extremity leads. Pilsicainide reduced ST-segment elevation in this patient, although class Ic antiarrhythmic drugs usually increase ST-segment elevation in patients with Brugada syndrome [5]. Autonomic nervous agents including atropine, acetylcholine, propranolol, and isoproterenol did not affect ST-segment elevation at all in this patient.

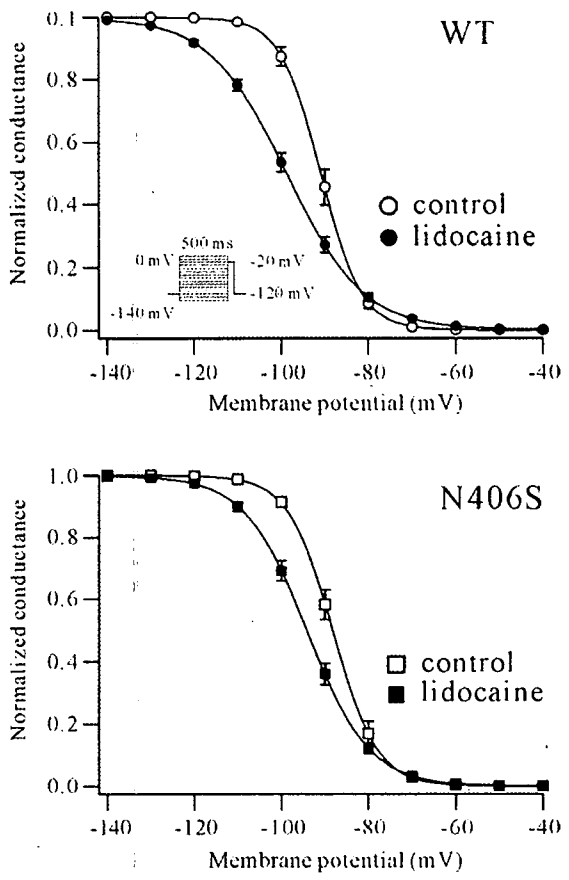

Fig. 2. Effects of lidocaine on steady-state availability of WT and N406S channels. Steady-state availability of channels was measured (Methods) in absence and presence of lidocaine. Averaged steady-state availability curves are shown in absence (circles) and presence of lidocaine (100 μM, squares). Graphs show normalized current plotted against conditioning pulse voltage. Smooth lines are according to $I/I_{max}=1/(1+\exp((V-V_{1/2})/k))$. V is conditioning potential. $V_{1/2}$ is voltage for which half the channels are available, and k is a slope factor. $V_{1/2}$ (mV) for WT is −90.9±1.1 for control, −99.6±1.4 with lidocaine; $V_{1/2}$ (mV) for N406S is −88.2±1.1 for control, −94.2±1.1 with lidocaine; $n=9$ cells per condition.